

{Continental Shelf Research}

Impacts of combined overfishing and oil spills on the plankton trophodynamics of the West Florida shelf over the last half century of 1965-2011: A two-dimensional simulation analysis of biotic state transitions, from a zooplankton- to a bacterioplankton-modulated ecosystem.

by

J.J. Walsh, J.M. Lenes, B. Darrow, A. Parks, and R.H. Weisberg

College of Marine Science, University of South Florida, St. Petersburg, FL 33701

Abstract

Over 50 years of multiple anthropogenic perturbations, Florida zooplankton stocks of the northeastern Gulf of Mexico declined ten-fold, with increments of mainly dominant toxic dinoflagellate harmful algal blooms (HABs), rather than diatoms, and a shift in loci of nutrient remineralization and oxygen depletion by bacterioplankton, from the sea floor to near surface waters. Yet, lytic bacterial biomass and associated ammonification only increased at most five-fold over the same time period, with consequently little indication of new, expanded “dead zones” of diatom-induced hypoxia. After bacterial lysis of intact cells of these increased HABs, the remaining residues of zooplankton biomass decrements evidently instead exited the water column as malign aerosolized HAB asthma triggers, correlated by co-travelling mercury aerosols, within wind-borne sea sprays. To unravel the causal mechanisms of these inferred decadal food web transitions, a 36-state variable plankton model of algal, bacterial, protozoan, and copepod component communities replicated daily time series of each plankton group’s representatives on the West Florida shelf (WFS) during 1965-2011. At the lower phytoplankton trophic levels, 52% of the ungrazed HAB increments, between 1965-1967 and 2001-2002 before recent oil spills, remained in the water column to kill fishes and fuel bacterioplankton. But, another 48% of the WFS primary production then left the ocean’s surface as a harbinger of increased public health hazards during continuing sea spray exports of salts, HAB toxins, and Hg poisons. Following the *Deepwater Horizon* petroleum releases in 2010, little additional change of element partition among the altered importance of WFS food web components of the trophic pyramid then pertained between 2001-2002 and 2010-2011, despite when anomalous upwelled nutrient supplies instead favored retrograde benign, oil-tolerant diatoms over the HABs during 2010. Indeed, by 2011 HABs were back, with biomass accumulations equivalent to those found in 2001.

1. INTRODUCTION

Reoccupation in August 2010 of a NEGOM cross-shelf section off Panama City, Florida, sampled (Jochens and Nowlin, 2000) earlier during August 2000 (Fig. 1), may have provided a partial answer to what was the cause of anomalous phytoplankton accumulations there by August 2010 of as much as ~ 5.0 ug chl l^{-1} above prior background levels during 2002-2009 (Hu et al., 2011), in this part of the WFS. Based on student t-test criteria, there were no significant differences in the phosphate contents of the water column there during August 2000 and 2010 (Fig. 2a). Except for significant depletion of nitrate within the aphotic zone of 500-1000 m depths, due to bioremediation of the *Deepwater Horizon* [DWH] fossil carbon substrates by aerobic denitrifying bacterioplankton (Fig 2b), there was no difference in the realized interdecadal stocks of this other “new” nitrogen nutrient within the euphotic zone during August 2000 and 2010. Thus, any decadal changes of bottom-up controls of at least P- and N-limitation were unlikely causes of phytoplankton population increments found after the *DWH* oil spills.

Moreover, dinoflagellate *Pyrocystis lunula* bioassays of possible deleterious phytoplankton responses to oil contaminants and trace metal poisons (Okamoto et al., 1999; Heimann, et al., 2002; Craig et al., 2003; Ozhan et al., 2014) then found there that any inhibitory impacts within the euphotic zone at a depth of 2 m were only $\sim 6.2\%$ of potential growth during August 2010 at station DSH08 on the 1050-m isobath (Paul et al., 2013). Yet, significant decadal increases of both ammonium (Fig. 2c) and the bulk DON within the euphotic zone at station DSH08 during August 2010, as well as later in May 2011, required an ongoing supply of autotrophic organic matter to fuel this decomposition process of the near-surface water column above the upper continental slope. Furthermore, *DWH* oils did penetrate inshore to WFS beaches that year (McDaniel et al., 2015), where a data-rich time series instead prevailed (Fig. 3).

As part of a continuing overfishing-induced trophic cascade, begun in 1965 (Walsh et al., 2011; 2015a), copepod grazing pressures had been reduced to $<10\%$ of previous removals of phytoplankton prey of varying palatabilities by 2010, at the start of the deleterious *DWH* oil spills. The same accumulation of ungrazed phytoplankton, lysed (Lenes et al., 2013) at HAB demises (Fig. 3) for export as aerosolized asthma triggers together with co-travelling mercury aerosols (Walsh et al., 2015a), could also have provided the particulate fuel for observed decadal increments of ammonifying bacterioplankton activities and their recycled nitrogen end product (Fig. 2c). Finally, removal of usual chronic zooplankton fecal pellet vectors of phytodetritus to the sea

bottom, compared to those of acute episodic oil-coagulated marine snow, may have shifted loci of prior element remineralizations to the near surface water column. There, small slow sinking phytoplankton cells, no longer sheathed in fecal pellets and marine snows of faster settling velocities, were less likely to have exited the surface water column, before decomposition to form pools of ammonium over 2000-2010.

Given these observed decadal temporal changes of seaward boundary conditions along the shelf-break, as well as inter-annual variations of onshore fluxes of dissolved and particulate matter due to varying rates of upwelling (Weisberg et al, 2014), did shelf-wide constituents of the WFS exhibit similar chronologies? For example, the decadal stocks of silicate at the shelf-break off Panama City had also not changed significantly within the euphotic zone between 2000 and 2010 (Fig. 2d).

Yet, upwelling during 2010 was anomalously persistent that year, like in 1998 (Weisberg and He, 2003; Walsh et al., 2003; Weisberg et al., 2014; Walsh et al., 2015a), such that despite inferred relaxation of grazing pressures on the WFS, the accumulation of toxic dinoflagellate HABs of *Karenia brevis* were negligible in 2010 (Fig. 3), i.e. even smaller than those of 1998. Instead, more oil-tolerant diatom (Ostgaard et al., 1984) winners of the 2010 WFS phytoplankton competition were 1.4-3.4 fold more resistant that year to total petroleum and polycyclic aromatic hydrocarbons of Louisiana sweet crude oil of *DWH* origins, than *P. lunula* (Ozhan et al., 2014), once presumed Si-limitation was again alleviated (Walsh et al., 2003).

Accordingly, to test these hypotheses and answer the question of concurrent chronologies at both sea and land boundaries of the WFS, we applied here the same model (Walsh et al. 2015a), used in recent short term assessments of both particle fall-out and potential sea spray exports of marine HAB and Hg aerosols, to now examine the implications and consequences of long-term plankton chronologies of the inner WFS (Fig. 3), between the coastline and the 50-m isobath, off Sarasota, Florida (Fig. 1).

2. METHODS

2.1 Model structure

This model's state vector consisted of a suite of 29 explicit and 7 implicit variables. In its present heuristic mode, the daily food web interactions of the WFS during three cases of the 1965-

1966, 2001-2002, and 2010-2011 model scenarios (Fig. 6) were defined in our present two dimensional model by a total of 36 state variables. They began with physical and chemical habitats of: {1} wind forcing; {2} temperature; {3} salinity; resultant {4} vertical K_z and {5} horizontal K_x mixing coefficients as parameterizations of local and lateral physical exchanges of dissolved and particulate matter; {6} spectral light; {7} colored dissolved organic matter (CDOM) of sloppy copepod feeding origin; dissolved {8} iron; {9} di-nitrogen gas; {10} nitrate; {11} ammonium; {12} organic nitrogen (DON); {13} silicate; {14} phosphate; {15} organic phosphorus (DOP); and {16} organic carbon (DOC).

Most of these simulated substrates were used by {17} ammonifying lytic bacterioplankton; as well as by {18} nitrifying bacterioplankton, with no formulations of either aerobic denitrifying bacteria, or sulfate-reducing microbes (Walsh et al., 2015a). Both of these pelagic heterotrophs competed for use of the nutrients against; chlorophyll-containing small diatoms {19} *Skeletonema costatum*; and large diatoms {20} *Rhizosolenia setigera*; {21} autotrophic microflagellates *Isochrysis galbana*; the precursor {22} diazotrophs *T. erythraeum* of toxic {23} dinoflagellate *K. brevis* HABs; in contrast to the non-toxic {24} *Cochlodinium polykrikoides* dinoflagellates; and {25} mixotrophic microflagellates *Paraphysomonas* spp.

But, note that the mean half-saturation constant k_s for assimilation of CO_2 by six functional groups of autotrophic phytoplankton (small and large diatoms, diazotrophs, toxic and non-toxic dinoflagellates, microflagellates) was only 1.2 $\mu\text{mol C l}^{-1}$ (Table 2), i.e. equivalent to 1.5 $\mu\text{mol C l}^{-1}$ for the mixotrophic microflagellates *Paraphysomonas* spp. of the model. Furthermore, the usual stocks, S , of dissolved CO_2 within the euphotic zone were 10-15 $\mu\text{mol C l}^{-1}$ (Burkhardt et al., 1999; Riebesell, 2004), such that minimal carbon-limitation of all phytoplankton would prevail at ~87-90 % of the potential realized growth rate, g , employing the usual Michaelis-Menten definition of substrate uptake kinetics [$g = g_{\max} (S/(k_s + S))$]. Most marine phytoplankton were capable of using bicarbonate (HCO_3) carbon substrates as well (Nimer et al., 2008), so accordingly carbon-limitation of the phytoplankton was ignored in the model, but not that of the bacterioplankton.

In the anabolic non-linear terms of each state equation, gP , the g_{\max} were maximal rates of nutrient uptake, photosynthesis, and growth of P biomass of phytoplankton, bacterioplankton, tunicates, ciliates, herbivorous copepods, and omnivorous copepods, in units of equivalent carbon

stocks, at each time step. Then, S were the respective light irradiance and nutrient, labile DOC, prey concentrations. In the last catabolic term of food web closure of the model, i.e. loss of copepods to chaetognath and scyphomedusa predators, S replaced P , such that predation was a function of prey copepod biomass S and also of the half-saturation constants k_s for the invertebrate carnivores (Reeve, 1980; Moller and Rissgard, 2007), but not of their biomasses, since they were implicit state variables.

Within the upper 50 m of the GOM basin off Louisiana, the labile carbon concentrations, S , of glucose sugars were instead $\sim 0.007 \text{ umol C l}^{-1}$ during 1996 (Skoog et al., 1999) of presumed ages of <10 years (Cherrier et al., 1999). By comparison, $\sim 270 \text{ umol C l}^{-1}$ of mainly refractory high molecular weight DOC occurred within the Mississippi River Delta (Gardner et al., 1996), in contrast to a global mean since 1994 (Ogawa and Tanoue, 2003) of $\sim 70 \text{ umol C l}^{-1}$ of much older oceanic DOC (Williams and Druffel, 1987). Using the k_s for the assimilation of labile DOC of $0.100 \text{ umol C l}^{-1}$ by bacterioplankton (Table 2), the observed GOM sugar substrate of $\sim 0.007 \text{ umol C l}^{-1}$, and the same Michaelis-Menten expression, about 93% of these simulated heterotrophic microbes would have been limited by available labile carbon stocks. Accordingly, sources of labile carbon in the model were “*slippery*” feeders at the herbivore and omnivore trophic levels, assuming whole ingestion of prey by bacteriophages, and ignoring DOC influxes from implicit carnivores, terrestrial runoff, and recent oil spills (Walsh et al., 2015a).

Cell lysis of *K. brevis* HABs was described in the model by two IF statements, concerned with critical masses of both accumulated dinoflagellates and ammonifying pelagic bacteria of the model (Lenes et al., 2013). We thus postulated that such a labile organic carbon substrate scarcity for bacterial predators increased phytoplankton susceptibility to lytic, particle attaching bacterioplankton (Azam and Malfatti, 2007; Zhang et al., 2007; Hunt et al., 2008; Nicolaisen et al., 2012), no longer content to utilize just DOM as free-living bacteria of the water column.

These C, N, P, Si and Fe-modulated lower heterotrophic and autotrophic levels of the model were eaten in turn: by {26} ciliates *Strobilidium spiralis*; {27} tunicates *Oithona dioica*; and copepods {28} *Temora turbinata* and {29} *Centropages velificatus*; subject to implicit predation by {30} chaetognaths *Sagitta hispida*; {31} moon jellies *Aurelia aurita*; and nearshore small adult pelagic fish stocks, dominated by the zoophagous Spanish sardine *Sardinella aurita* as decaying, HAB-killed {32} forage fish sources of recycled nutrients (Walsh et al., 2009), between

the coastline and the ~20-m isobath (Pierce and Mahmoudi, 2001). Some of the new highlights of the present model were thus explicit non-linear prey- and predator-dependent grazing rates, as well as egestion rates of fecal pellets by four explicit functional groups (ciliates *S. spiralis*; tunicates *O. dioica*; copepod herbivores *T. turbinata* and omnivores *C. velificatus*) of zooplankton (Table 1).

Finally, a benthic shunt of near-bottom remineralization (Darrow et al., 2003) recycled additional nutrient sources of decomposing phytodetritus and these combined zooplankton fecal pellets {33}, in use by the implicit benthic diatoms *Navicula* spp. {34}, grazed in turn by the implicit {35} macrobenthic oyster herbivores *Crassostrea virginica*. The heterotrophic components of the plankton model had units of equivalent particulate organic carbon (POC), nitrogen (PON), phosphorus (POP) and iron (PFe), whereas the phytoplankton biomasses had additional equivalent units of chlorophyll, and in the diatom cases, particulate silicon (PSi). The last implicit variable was the particulate mercury content of absorbed mercury {36} in diatoms (PHg), with a mercury content (Knauer and Martin, 1972) of 207 ng Hg g⁻¹ dw of the simulated larger *R. setigera* (Table 1) populations.

Since larval fishes were a minimal source of GOM copepod mortality (Dagg and Govoni, 1996), their impact on the WFS food web was ignored in computed hourly element exchanges among the model's state variables. These early life history stages of vertebrates fed on those copepod naupliar and copepodite stages (Baier and Purcell, 1997) of zooplankton, which were also presently unresolved by this model. Similarly, the oil poisonings of larval fishes (Carls and Rice, 1989) were presently neglected here. But, these larval fishes were also consumed by competing chaetognaths (Coston-Clements et al., 2009), eating both copepods and ichthyoplankton, such that the summary carbon budgets did consider their role in the plankton trophic pyramids of Table 2.

Yet, the surviving oil-poisoned, pesticide-poisoned, and Hg-poisoned copepod stocks of the WFS, after monthly net secondary productions within a trophic cascade, were not ignored. Instead, they were empirically imposed as part of the model's "known" interannual cross-shelf boundary conditions of herbivory, exerted by the four zooplankton state variables during 1965-1966, 2001-2002, and 2010-2011 (Tables 3-5). Their explicit losses were, in turn, non-linear Monod functions of both the net remaining zooplankton biomasses computed every hour and the prey half-saturation constants of food concentrations required by their invertebrate plankton and adult fish predators (Table 1).

2.2 Physical transports

Following an earlier 2-D biophysical model of much simpler biotic interactions on the WFS (O'Brien and Wroblewski, 1973), the vertical and lateral physical exchange processes were still described here by eddy coefficients K_z and K_x . The rich details of fully three-dimensional circulation models of oil (Liu et al., 2011a,b) and plankton (Weisberg et al., 2014; 2015a, b) dispersions over the WFS were beyond the scope of this already complex, present simulation study. Since values of K_z and K_x , like the advective fields, were dependent upon wind and buoyancy forcings (Mellor and Yamada, 1974), which were available for 1965-1966 (Joyce and Williams, 1969), 2001-2002 (Lenes et al., 2012), and 2010-2011 (Liu et al., 2011a,b), we instead used time-varying estimates of K_z over the water column of the 20-m isobath and of K_x between the 5-m and 45-m isobaths (Fig. 1).

The prior study had originally employed time-invariant respective mixing coefficients K_z and K_x of $\sim 1 \text{ cm}^2 \text{ sec}^{-1}$ and $\sim 1 \times 10^6 \text{ cm}^2 \text{ sec}^{-1}$, thought to be typical of WFS winter conditions, in that first 2-D cross-shelf model to effect turbulent transports (O'Brien and Wroblewski, 1973). Winter surface mixed layers extended to depths of >50 m in the GOM, effecting K_z of $\sim 50 \text{ cm}^2 \text{ sec}^{-1}$ (Walsh et al., 1989), while larger K_z values of $\sim 190 \text{ cm}^2 \text{ sec}^{-1}$ were estimated after other shelf wind events (Wroblewski and Richman, 1987). So, we instead assumed a conservative maximal winter value of $\sim 40 \text{ cm}^2 \text{ sec}^{-1}$ here, as used successfully in other prior WFS models (Lenes et al., 2012) to reflect resupply of allochthonous nutrients of shelf-break and estuarine origins.

With establishment of summer thermoclines, values of instead $\sim 1 \text{ cm}^2 \text{ sec}^{-1}$ for K_z were not uncommon, and used in other models (Falkowski et al., 1980; Harrison et al., 1983). Accordingly, here the model's summer minimal value of K_z was $1 \text{ cm}^2 \text{ sec}^{-1}$ to effect physical resupply of autochthonous recycled nutrients of biotic origins. When summer shelf circulations led to frontal regions, the associated K_x of lateral exchanges of allochthonous properties across these physical structures were then as small as $\sim 3 \times 10^5 \text{ cm}^2 \text{ sec}^{-1}$ (Klein, 1986), compared to nominal values of $\sim 3 \times 10^6 \text{ cm}^2 \text{ sec}^{-1}$ (Ketchum and Keen, 1955; Riley, 1967; Stommel and Leetma, 1972) used in more of our past models (Coachman and Walsh, 1981; Walsh et al., 1997). Again, we employed a seasonal range, but now that of a ten-fold difference between summer and winter lateral exchanges represented by K_x , compared to a 40-fold change in vertical mixing effected by K_z .

From one year to the next, within these seasonal ranges, the daily persistence of the model's specific values of K_z and K_x was also modulated by both wind and buoyancy, where the observed WFS temperatures and salinities were indices of past Loop Current penetration onto the shelf over 1965-2011, seen during the many cruises (Fig. 1). By conservations of mass and momentum, of course, such alterations of hydrographic properties also reflected offshore transports of water parcels and their constituents, forced by the Loop Current, local runoff, heating, and regional wind fields, with all the biotic rate processes of the model also regulated by temperature (Table 1). Time-dependent boundary conditions were next specified at these isobaths to represent both physical exchanges of dissolved nutrient and particulate micro-algal and bacteria state variables of the model, in relation to "known" interannual amounts of incident radiation and the surviving monthly stocks of planktonic herbivores and omnivores, transported by mixing and harvested by carnivores.

2.3 Boundary conditions

Information from microscope counts of copepod nauplii in bottle casts, as well as of zooplankton adults and their larval stages from net tows and pump samples, were obtained with varying mesh sizes. These data were combined to specify surviving monthly cohorts of herbivore carbon biomasses at the 5-m and 45-m isobaths of the WFS during the Hourglass, ECOHAB, and C-IMAGE cruises (Fig. 1). Basically, the seasonal zooplankton carbon stocks on the inner WFS of *Centropages*, and *Strobilidium* had each already declined ten-fold from 1965-1966 to 2001-2002, before the oil spills of 2010-2011 began (Tables 5-7). In contrast, carbon biomasses of *Temora*, and *Oikopleura* remained about the same between 1965 and 2002, with then ten-fold decrements after 2010.

2.4 Validation data

As indicated by the open circles and triangles of Figures 4-10, fidelities of the computed state variables were estimated from observations of: nitrate and ammonium (Jochens and Nowlin, 2000; USF data); cell counts of *Trichodesmium* and *K. brevis* (FWRI data); *Rhizosolenia* spp. (Saunders and Glenn, 1969; Jurado et al., 2007); *S. costatum* (Saunders and Glenn, 1969); *C. polykrikoides* (FWRI data); bacterioplankton (Pomeroy et al., 1995; Jones et al., 2010); *O. dioica* (FWRI; Lester et al., 2008); *C. velificatus*, *T. turbinata* (King, 1950; Turner, 1984, 1987; Kleppel et al., 1996; Lester et al., 2008; Walsh et al., 2015a); and ciliates (King, 1950; FWRI; Lynn et al.,

1991). Since this model was in a heuristic, rather than an operational, mode, sensitivity analyses of model infidelities, compared to observations, were retained to illustrate inadequate results, due to both incorrectly assumed maximal nitrifications rates of bacterioplankton and trophodynamics of micro-zooplankton, in already complex descriptions of interacting WFS plankton populations.

3. RESULTS

3.1 Nutrients

During summer on the WFS, once stratification of the water column curtailed vertical mixing supplies of allochthonous nutrients as nitrate, the increased importance of autochthonous recycled nutrients was observed previously (Walsh et al., 2003) and simulated here over 1965-2011 (Fig. 3). Ammonium of the other dissolved inorganic nitrogen [DIN] pool became particularly important, as well as labile urea, glutamate, and amino acids of the DON pools, all utilized by *K. brevis* (Baden and Mende, 1979; Steidinger et al., 1998; Bronk et al., 2004). The recycled nitrogen stocks (Fig. 4) were initially of *Trichodesmium* origin (Fig. 5a) for correct prediction of prior summer onsets of *Karenia* HABs during 2001 (Fig. 5b). The four-fold increment of observed June-August recycled nitrogen pools between 1999 and 2011 off Sarasota (open square symbols of Fig. 4), like the same decadal increases of August bacterial ammonium remineralization rates and pools found within near surface waters at the shelf-break off Panama City during 2000 and 2010 (Fig. 2), reflected a regime shift to an unbalanced plankton state of the GOM, after overfishing, oil spills, and releases of heavy metals and pesticides reduced zooplankton fecal pellet vectors to the sea floor (Walsh et al., 2015a).

While, the total simulated DIN matched the combined observations of nitrate and ammonium, the present scenario of faster nitrification rates overestimated the former nitrogen form and underestimated the latter. Here, we used a maximal nitrification rate at 30°C of 0.30 day⁻¹ (Table 1), compared to a prior smaller parameter value of 0.05 day⁻¹ in an earlier 3-D model (Walsh et al., 2006). Here, no considerations were now made of either additional CO₂ carbon-limitation, or more importantly light-limitation, of the zero sum exchange between oxidation states of DIN (Ward, 1996), by the present simulated nitrifying bacterioplankton (Fig. 4).

Field observations of realized nitrification rates within a similar ecosystem of the northwestern Mediterranean Sea found near shore ammonium oxidation rates at 35.0 psu in May surface waters of 0.23 umol N l⁻¹ day⁻¹ by a nitrifying bacterial population of ~2.6 x 10⁷ cells l⁻¹,

i.e. ~2% of the total bacterioplankton, at a thermal Q_{10} of 2.7 (Bianchi et al. 1994; 1999), similar to the model's temperature estimate (Table 1). Given a bacterial cellular nitrogen content of ~1 femtomol N cell⁻¹, or 13.7×10^{-9} ug N cell⁻¹ (Fagerbakke et al., 1996; Fukuda et al., 1998; Vrede et al., 2002), the specific nitrification rate would have then been ~0.03 day⁻¹ in a May CDOM-shaded habitat of ~14°C off the Rhone River (Bianchi et al. 1994; 1999), or perhaps 0.08 day⁻¹ at 28°C on the WFS. Accordingly, a more realistic slower rate of simulated ammonium oxidation would have reversed the respective amounts of ammonium and nitrate accumulations within the DIN pools of this version of the model (Fig. 4).

The previous smaller simulated nitrification rate of 0.05 day⁻¹ represented biotic autochthonous sources of nitrate, in contrast to allochthonous physical supplies of slope nitrate pools within fully 3-D circulation fields (Walsh et al., 2003; 2006). But, given the focus here on remineralization processes of nitrogen and thus the simplicity of cross-shelf nitrate exchanges in this 2-D model, increased model fidelity would have also required a more complex 3-D version, now under formulation, to more accurately again import nitrate stocks from the WFS shelf-break (Walsh et al., 2003; 2006). Yet, once the initial ammonium sources from commensal diazotrophs (Fig. 5a), decomposing dead fish, and zooplankton excretion of this model came into play, they now effected here the required larger amounts of fall maintenance nutrients for HABs of *K. brevis* (Fig. 5b), estimated in previous nitrogen isotope budgets (Walsh et al., 2009).

Use of ammonium for partial growth of the other simulated phytoplankton replicated observations of: large and small *Rhizosolenia* and *Skeletonema* spp. diatoms (Fig. 6); another non-toxic dinoflagellate *Cochlodinium* spp. (Fig. 7); and *Isochysis* spp. microflagellates, all in competition with both the HABs (Fig. 5) and the nitrifying bacterioplankton (Fig. 8). For example, the present model results also replicated the seasonal six-fold carbon increments of accumulated biomass of *K. brevis* in October of most years (Fig. 3), compared to smaller summer amounts of precursor diazotroph populations in August (Figs. 5a,b), due to additional harvests of zooplankton and poisoned fish sources of nitrogen by the toxic dinoflagellates.

3.2 Phytoplankton

As a beneficiary of those nutrient supplies, recycled from: **1**) the diazotroph colonies (Fig. 5a); **2**) zooplankton excretion; and **3**) decaying fishes killed by HABs, the simulated large populations of *K. brevis* followed (Fig. 5b) those of the model's *Trichodesmium* precursors during

every year, except 2010 (Table 6). Then, both small diazotroph and HAB populations were predicted (Table 6), when diatoms instead dominated the WFS in 2010, like in 1998 (Walsh et al., 2003; 2015a), with few HABs noted (Fig. 3). As a consequence of the anomalously decadal strong bottom-up supply of nutrients via upwelling in 2010 (Weisberg et al., 2014) to fuel successful oil-tolerant diatom competitors, the contiguous downstream offshore flows off Sarasota also “*washed out*” these siliceous winners, leaving behind little accumulated biomasses of larger diatoms on the central WFS that year (Fig. 6e). Otherwise, following top-down, ten-fold reductions of the herbivore stocks on the inner shelf between 1965-1966 and 2011 (Tables 3-5), the simulated annual net accumulations of *K. brevis* had doubled from similar amounts of 90-91 $\mu\text{mol C l}^{-1}$ during 1 October 1965-1966 to 177 $\mu\text{mol C l}^{-1}$ in October 2001 (Table 6).

By contrast, the model’s other simulated responses to these changed nutrient and grazing constraints was just a two-fold increase of fall accumulations of *R. setigera* biomass by 1 September 2011 (Figs. 6a, c, e), compared to their computed abundances on that date in 1966 and 2002. Yet, the imposed boundary conditions of presumably oiled herbivorous *Temora* spp. on the WFS inshore 5-m isobath were those of ten-fold less biomass of 0.01 $\mu\text{mol C l}^{-1}$ in September 2010, compared to 0.10-0.14 $\mu\text{mol C l}^{-1}$, estimated from naupliar and adult copepod stocks measured in the same month of 1965 and 2001 (Tables 3-5).

Despite smaller grazing losses, continued silicon-deprivation had occurred as one of the bottom-up controls in the model, once *R. setigera* exceeded its own carrying capacity, upon initial relaxation of top-down grazing pressures. Between September 1965 and 1966, carbon biomasses of *Rhizosolenia* had declined from $\sim 4.5 \mu\text{mol C l}^{-1}$ to $\sim 0.5 \mu\text{mol C l}^{-1}$, while the stocks of *S. costatum* were the same $\sim 0.3 \mu\text{mol C l}^{-1}$ from April 1965 to April 1966 (Table 6). The larger diatoms remained at the reduced low population levels during 1999 and 2000 (Fig 6c), when validation data (Jurado et al., 2007) were obtained during those years at the 20-m isobath off Cape Sable (the inverted open triangle symbol of Fig. 1).

The half-saturation constant for silicate uptake by the simulated *Rhizosolenia* state variable was two-fold greater than that of the model’s smaller diatom *S. costatum* (Table 1). In prior laboratory studies, *Rhizosolenia fragilissima* had ten-fold more silica per cell in their frustules than *S. costatum* (Paasche, 1980), such that the former *R. setigera* would have also suffered silica-limitation much faster than these other diatoms. As a consequence of less stringent bottom-up

control, *S. costatum* populations did not show similar interannual variability of biomass accumulations (Figs. 6b,d,f). A nutrient reprieve for these larger diatoms occurred, after the anomalous upwellings of 2010, with two-four fold seasonal increments of *R. setigera* realized in the model during 2010 and 2011 (Table 6), fueling, in turn, an increment of *Temora* herbivores by 2011, as well (Fig. 10e).

Without such silica-limitation of these microalgal prey Hg-carriers to zooplankton and higher trophic levels, the simulated long-term increases of carbon and mercury biomasses of the model's *R. setigera* populations (Table 6) would have each been greater. When the model's seasonal maxima of these edible diatoms increased from 0.5 $\mu\text{mol C l}^{-1}$ in September 1966 to 1.6 $\mu\text{mol C l}^{-1}$ by September 2001 (Table 6), the observed mercury body burdens of the WFS *Scombermorus* mackerels had also increased from 232 to 409 ng Hg g^{-1} dw over a similar time period (Adams and McMichael, 2007). To place these statements on a comparative per unit volume basis, however, for estimates of decadal food web transfers of Hg on the WFS, from diatoms to edible piscivores, some additional assumptions and biomass conversions were made.

During September 2001, the computed 1.6 $\mu\text{mol C l}^{-1}$ of *Rhizosolenia* diatoms (Table 6), or 0.36 $\mu\text{g chl l}^{-1}$ was equivalent to 20.0 $\mu\text{g dw l}^{-1}$, assuming a C/chlorophyll weight ratio of 53 for *R. setigera* (Mullin et al., 1966; Stauber and Jeffrey, 1988), and that chlorophyll pigments were 1.8% of micro-algal dry weight (Dolan et al., 1978). Then, the mercury content of these WFS diatom populations would have been 4.14 $\mu\text{g Hg l}^{-1}$, further assuming that year-round diatom populations in the California Current were “*typical*”, with a mean monthly mercury body burden of 207 ng Hg g^{-1} dw (Table 1) throughout 1971 (Knauer and Martin, 1972).

Finally, during October 2001, an estimated fish spacing of one m^{-2} in the WFS (Walsh et al., 2006) suggested a fish concentration above the 10-m isobath of one ~7 year-old female king mackerel *Scombermorus cavalla* of ~30 kg ww, or 7.5 g dw l^{-1} . A mercury body burden of the mackerels then of 409 ng Hg g^{-1} dw (Adams and McMichael, 2007) yielded a possible mercury content of 307 $\mu\text{g Hg l}^{-1}$ for these WFS piscivore fish populations. This bioaccumulation factor of ~75 fold in 2001 was similar to that measured of ~70-fold on the WFS, from detritus to piscivore lane snappers *Lutjanus synagris* during 1995 (Kannan et al., 1998).

Reduced grazing losses and no silicon demands had also led to successful competition by *K. brevis* during most years on the WFS (Walsh et al., 2015a), resulting in a mean accumulation

instead during August-December 2001 of a much larger $\sim 5 \times 10^6$ cells l^{-1} (Fig. 3), or $\sim 50 \mu g$ chl l^{-1} and $125 \mu mol$ C l^{-1} of the toxic *K. brevis* (Table 1) with a chlorophyll content of 100 pg chlorophyll cell $^{-1}$ and a C/chl weight ratio of 30 (Walsh et al., 2001). However, most of this primary production by *K. brevis* was not passed up the food web, since grazing by WFS zooplankton herbivores and omnivores on the red tides was then small, after the ten-fold reductions of the individual biomasses of zooplankton groups (Table 2).

In contrast to the summer-fall bloomings of as much as $\sim 150 \mu mol$ C l^{-1} of *K. brevis*, the other competitor *Cochlodinium* sp. behaved instead like the diatom *S. costatum*, but with winter blooms of just 3-5 μmol C l^{-1} of this second dinoflagellate simulated by January 2002 and 2011 (Figs. 7b, c). Moreover, these simulated and observed stocks of *Cochlodinium* sp. during 2010-2011 on the WFS were \sim five-fold less than those found in the adjacent estuaries during March 2011 (Fig. 7c). Such model results indicated that: (1) this eutrophic dinoflagellate, with large half-saturation constants for nutrient uptake (Table 2), was indeed a poor competitor on the WFS against *K. brevis*, adapted instead for oligotrophic habitats, and (2) the WFS had not yet been eutrophied, seaward of the mouths of the estuaries, despite popular convictions among some proponents of reduced nutrient loadings to Florida's coastal waters (Walsh et al., 2011).

If all of the July microflagellates counted by Karen Steidinger (*personal communication*) during the HOURGLASS cruises on the central WFS during 1965-1966 (Fig. 1) were typical of photosynthetic *I. galbana*, with a carbon content of ~ 3 pmol C cell $^{-1}$ (Thompson et al., 1992), phytoplankton stocks of $\sim 0.3 \mu mol$ C l^{-1} of autotrophic microflagellates would have been other food available to the dominant GOM ciliates, e.g. *Strombidium* and *Strobilidium* spp. (Liu et al., 2005). But, the ciliates *S. spiralis* had a half-saturation constant k_s of $\sim 8 \mu mol$ C l^{-1} for *I. galbana* of ~ 3 microns size (Verity, 1991), such that the realized ciliate summer growth rate g_s would have been only 4% of the potential maximal rate g_{max} .

In contrast, the k_s for consumption of *I. galbana* by larval polychaete competitors (Table 2) *Mediomastus fragile* was $\sim 5 \mu mol$ C l^{-1} (Hansen, 1993), allowing an intermediate g_s of about 6% of their potential maximum growth rate. Furthermore, the tunicates *O. dioica* of an average gelatinous house size had a half-saturation constant of $\sim 4 \mu mol$ C l^{-1} for *I. galbana* (Acuna and Kiefer, 2000). Such a greater affinity for consumption of small microflagellates by tunicates would

have provided these gelatinous microzooplankton with a two-fold competitive advantage over the ciliates, realizing instead larger g_s of 8% g_{max} , at the same prey concentration.

Yet, laboratory populations of *I. galbana* had only a growth rate of 3.1 day⁻¹ at 30°C (Hobson et al., 1979; Herzig and Falkowski, 1989; Thompson et al., 1992). Whereas at 13°C, other laboratory cultures of three genera of ciliates exhibited a mean suboptimal growth rate of 0.9 day⁻¹, while eating *I. galbana* (Strom and Morello, 1998). Upon assuming a temperature Q₁₀ (Table 2) of ~2.6 (Nielsen and Kiorboe, 1994), such WFS ciliate populations at sufficient prey abundances could have instead displayed a maximal growth rate of ~7.0 day⁻¹ at 30°C, i.e. two-fold larger than that of the autotrophic microflagellates. Thus, like silicon-limitation of ungrazed *Rhizosolenia* populations, the WFS ciliates may have suffered prey-limitation by overharvested microflagellates, once copepod omnivores no longer ate ciliates during the trophic cascade.

The tunicate *O. dioica* had a smaller growth rate of ~2.0 day⁻¹ at 20°C in the laboratory (Troedsson et al., 2002), with a Q₁₀ of 1.7 (Gorsky et al., 1987), such that their food-replete growth rate would have been just ~3.4 day⁻¹ at 30°C on the WFS (Table 2), similar to some field observations within the upstream Caribbean Sea off Jamaica (Hopcroft et al., 1998). Given these relative growth rates, both ciliates and tunicates, no longer eaten by copepod omnivores during oil spills and trophic cascades, would have quickly stripped microflagellates from the water column. Thus, onsets of food limitation would also have soon prevailed, with the faster-growing ciliates favored to win the outcome of microzooplankton competition within oil-free areas of the GOM, based on the model's "rules of engagement" (Table 1), in which the ciliate protozoans also had a bacterial food supplement, unlike the tunicates.

3.3 Bacterioplankton

The model's bacterioplankton did not require light for their anabolic processes, but they competed against the GOM phytoplankton for utilization of Fe, NH₄, DON, PO₄, and DOP (Table 1). In terms of validation data, ~3.0 x 10⁹ cells l⁻¹, or only 0.6 µmol C l⁻¹, of observed total bacterioplankton were found on the WFS along the 20-m isobath (Pomeroy et al., 1995) during the negligible HAB of June 1993 (Fig. 3). Then, small populations of the heterotrophic and autotrophic plankton may have both perhaps been consequences of earlier seasonal summer bacterial-induced lytic termination of the HAB carbon sources that year. Accordingly, few intact algal substrates would have survived by the fall for the bacterioplankton to lyse.

Yet, during the large HAB of September 2001 (Fig. 3), 2-4 fold greater bacterial populations of $1.0\text{-}3.5 \mu\text{mol C l}^{-1}$ were observed and simulated (Fig. 8b) above the same isobath. This larger bacterial community consisted mainly of: ~39% gammaproteobacteria, represented by *Pseudomonas* spp.; 22% cytophaga/flavobacterium/bacteriodetes, represented by *Cytophaga* spp.; and 12% alphaproteobacteria represented by algicidal *Roseobacter* spp. (Jones et al., 2010). Recall that the assumed ecophysiological properties of the model's bacterioplankton (Table 1) were mainly those of *Pseudomonas* spp., except for the very fast growing nitrifiers *Nitrosomonas*.

Ciliates were thought to be direct bacterivores (Bernard and Rassoulzadegan, 1990), with a maximal growth rate of 0.5 day^{-1} for *Strombidium* spp. at 15°C and a half-saturation constant k_s of $0.2 \times 10^{10} \text{ bacterial cells l}^{-1}$, or $\sim 60 \mu\text{mol C l}^{-1}$ of *Vibrio natriegens* (Ohman and Snyder, 1991). Similarly, a benthic ciliate *Strombidium sulcatum* had a half-saturation constant of $0.6 \times 10^{10} \text{ cells l}^{-1}$, or $\sim 180 \mu\text{mol C l}^{-1}$ (Fenchel and Jonsson, 1988; Bernard and Rassoulzadegan, 1990). However, since the observed bacterioplankton stocks on the inner WFS were only $0.6\text{-}3.5 \mu\text{mol C l}^{-1}$ (Fig. 8) along the 20-m isobath (Pomeroy et al., 1995; Jones et al., 2010), the pelagic ciliates were unlikely to have directly derived much of their nutrition from the heterotrophic base of this microbial loop, i.e. perhaps $\sim 1\text{-}6\%$ during the continuing WFS cascade.

Nevertheless, a five-fold increment of observed total bacterial biomass along the 20-m isobath of the inner WFS, between June 1993 and September 2001 (Pomeroy et al., 1995; Jones et al., 2010), was consistent with the inferred increases of ammonifiers at the shelf-break off Panama City during August 2000 and 2010 (Fig. 2d). Moreover, experimental trophic cascades of increments of nitrifying bacterioplankton were also caused by removal of aquatic bacterivores in Lakes Huron and Erie (Lavrentyev et al., 1997). Here, similarly, we suggest that a ten-fold reduction of the simulated *Centropages* copepod predators (Figs. 10b, d) on ciliates, between 1965-1966 and 2001-2002, initially relaxed predation pressures on the protozoans. But, once these ciliates were subject to subsequent prey-limitation, in turn, by over-grazed microflagellates, like the silica-limitation of the larger diatoms *Rhizosolenia*, another ten-fold decline of simulated ciliate omnivores *Strobildium* ensued between 1965-1966 and 2001-2002 (Figs. 9b, d). With minimal protozoan bacterivores on the WFS to harvest bacterial prey populations of both ammonifiers and nitrifiers, the microbes would have consequently increased – as observed between 1993 and 2001 – QED.

Furthermore, a 10% transfer efficiency (Fath and Patten, 1998) was derived here from model results between prey items of omnivores and herbivores and time-lagged biomass accumulations of the latter higher trophic levels (Table 6). Application of the same rates of trophic transfers between each component of a GOM microbial loop (Table 2), using instead bacterial prey as a food source for copepod omnivores via intermediate heterotrophic ciliate transfers of energy and elements (Gifford and Dagg, 1988), resulted in even smaller amounts of ~1% of copepod nutrition derived from bacterioplankton. Finally, after two additional trophic steps to mackerel piscivore fish consumers [bacterioplankton → ciliate → copepod omnivore → clupeoid zooplanktivore → mackerel], these carnivores would have derived only 0.01% of their required food from secondary production of the bacterioplankton.

Respiration costs were associated in the model with both initial utilization by bacterioplankton of labile DOC substrates, and their passage through ciliates, as well as by microflagellates eaten by tunicates, and pelagic diatoms eaten by copepods. Implicit bacterial activities in the sediments also had carbon respiration taxes during regeneration of nutrients, consumed by *Navicula* benthic diatoms and, in turn, by *Crassostrea* oysters, with other associated respiration costs. But, since no sulphate-reducing, methylating bacteria (Compeau and Bartha, 1985; Choi and Bartha, 1994; Deveraux et al., 1996) of the sediments were present in this model (Walsh et al., 2015a), their respiration and the distinct pools of recycled inorganic Hg and organic MeHg were ignored here.

3.4 Microzooplankton

Although *O. dioica* houses were of similar ~700 microns size to other mesozooplankton crustacean herbivores and omnivores in some cases, e.g. *Paracalanus parvus* and *Acartia tonsa*, they were considered here to be functional microzooplankton of the model (Figs. 9a, c, e), since they usually ingested picoplankton particles of <5 microns (Troedsson et al., 2002; Vargas and Gonzalez, 2004; Lombard et al., 2005). Similarly, the ~50 microns sized *Strobilidium* ciliates of the model (Figs. 9b, d, f) consumed the same small microflagellate prey, as well as bacterioplankton (Fig. 8). In contrast, some of the food supplies for copepod herbivores and omnivores were the net phytoplankton, i.e. the >25 microns chain size of colonial diatoms and the larger dinoflagellates *K. brevis* of 20-40 microns width, as well as the smaller ciliates. But, like the microbial heterotrophic food chain leading to omnivore copepods, e.g. *Centropages* spp. (Fig. 10), these

consumers also ate tunicates [salps, or larvaceans], such as appendicularians *O. dioica* (Sommer et al., 2003; Lopez-Urrutia et al., 2004) in another parallel model food chain [microflagellate → tunicate → copepod omnivore → clupeoid zooplanktivore → mackerel].

Full impacts of GOM overfishing were not realized among these plankton communities until the 1980s. Then, zoophagous *S. aurita* and thread herring *Opisthonema oglinum*, feeding at the lower zooplanktivore trophic levels of forage fishes, replaced spring spawning grouper and snapper piscivores (Collins et al., 2001; Renan et al., 2001). Additionally, moon jellies *A. aurita* and sea nettles *Chrysaora quinquecirrha* at the same trophic level of these clupeoid forage fishes had also increased ten-fold between 1985 and 1997 on the Alabama shelf (Graham, 2001). Finally, a similar 7-fold increment of chaetognaths at this primary carnivore level had occurred in the Bay of Campeche over the same time period on the western side of the GOM (Guzman del Proo et al., 1986; Mille-Pagaza and Carillo-Laguna, 1999), as part of the Gulf-wide trophic cascades (Walsh et al., 2011; 2015a). As implicit plankton predators, without specification of their respective biomasses, the removals of adult copepod prey as part of the latter's mortality rates (Hirst and Kiorbe, 2002) were still different functions of the half-saturation rates (Table 1) for consumption of copepods by chaetognaths (Reeve, 1980) and medusae (Moller and Rissgard, 2007).

During the 1980s, all of these GOM zooplanktivores had increased food demands on smaller, post-cascade populations (Tables 3-5) of their prey, i.e. subsequently surviving dominant herbivores and omnivores in 2001-2002, before the *Deepwater Horizon* oil spills (Walsh et al., 2015a). Then, the major groups of larger zooplankton sizes were the tunicates *O. dioica* (Figs. 9a, c, e) and the copepods *T. turbinata* (Figs. 10a, c, e) and *C. vellificatus* (Figs. 10b, d, f), found (Lester et al., 2008) during the *ECOHAB* cruises (Fig. 1).

Of these two copepod genera (Fig. 10) of the same sizes, the simulated WFS zooplanktivore demands had greater predation impacts on the omnivores *C. vellificatus*, than on the herbivores *T. turbinata*, despite supplemental food supplies of tunicates and ciliates for the former as possible trophic upgrades of required fatty acids and sterols (Klein Breteler et al., 1999, 2004; Tang and Taal, 2005). In the Mediterranean Sea off Naples, Italy, *Centropages typicus* may also have been subjected to more predation losses than *Temora stylifera* (Di Capua and Mazzocchi, 2004), reflecting the greater fecundity rate of the former copepod (Kiorboe and Sabatini, 1995).

3.4.1 Ciliates

Using an average carbon content of 1.4 nmol C individual⁻¹ (Putt and Stoecker, 1989), the monthly observed biomasses of ciliates along the WFS, between Tampa Bay and Charlotte Harbor, from the HOURGLASS cruises (Fig. 1) exhibited a seasonal maximum of 47,645 ciliates l⁻¹, or ~66.7 μ mol C l⁻¹, during June 1965 and 1966 at the 5-m isobath (Table 3). By comparison, 1.0 μ mol C l⁻¹ of the protozoans occurred in those months above the 45-m isobath (Table 3). Given these time-dependent and spatially-variant boundary conditions, in relation to the simulated food supplies and population losses of the ciliates during horizontal and vertical mixing of their physical habitat, the model results yielded a monthly maximum of 12.0 μ mol C l⁻¹ of *Strobilidium* on 1 July 1965/1966 of the initial trophic cascade above the 20-m isobath (Table 6).

Such a simulated maximal WFS ciliate accumulation of prey biomass during 1965 and 1966 occurred 124 days before the model's successful growth of computed omnivore *Centropages* adults on 1 November 1965 and 1966. This accumulated copepod stock (Fig. 10b) of 1.28 μ mol C l⁻¹ (Table 6) represented a trophic transfer efficiency of 10% between two sets of omnivores: copepod predator and protozoan prey. Before simulated silica-limitation curtailed growth of *Rhizosolenia* spp. by 1 September 1966, their accumulated stock a year earlier of 4.30 μ mol C l⁻¹ on 1 September 1965 again yielded 0.46 μ mol C l⁻¹ of WFS *Temora* spp. by 1 May 1966 (Table 6). Thus, another trophic transfer efficiency of 10% was realized between instead phytoplankton prey and copepod herbivores of the model. Presumably, a large stock of *Rhizosolenia* spp. in 1964 had similarly fueled the same amount of computed biomass of 0.48 μ mol C l⁻¹ of *Temora* spp. on 1 May 1965 (Table 6), since no competing HABs then occurred earlier during 1964 (Fig. 3).

Furthermore, the model's imposed monthly surface temperatures on the ~20-m isobath of WFS during July-October 1965 and 1966 were a mean of 29.1°C (Joyce and Williams, 1969), still favorable for growth of these warm-water copepods (Hassett and Crockett, 2009), until a lethal limit above 30.0°C was obtained (Halsbank-Lenk et al., 2002). Given durations of ~12 days at 15.0°C for each of the usual isochronal eleven early life history stages (Di Capua and Mazzocchi, 2004) of both *C. typicus* and *T. stylifera* (6 naupliar and 5 copepodid phases) off Naples, Italy, the WFS juvenile stages would have lasted ~132 days, from nauplius to moulted adult female of each species, at the same temperature. But, with an overall Q₁₀ of 3.0 for growth of *Centropages* and *Temora* (Table 1), the early life history durations of both WFS populations may have been instead just ~44 days during summer temperatures for adults to emerge as prey for zooplanktivores, after

eating ciliates as the major menu item in the daily diet of the former, compared to mainly diatoms and dinoflagellates of the latter.

On 5 August 1992, for example, the observed diet of *C. velificatus* consisted then of 86% microzooplankton and 14% diatoms on the WFS (Kleppel et al., 1996). In contrast, *T. turbinata* was unable to catch GOM ciliates (Wu et al., 2010) with its filtering currents, effected by moving their mouth parts. Indeed, by the beginning of August 1992 on the WFS, the surviving facultative herbivores *T. stylifera* ate protozoans as the last resort (Kleppel et al., 1996), apparently preferring an equivalent amount of *K. brevis* (Turner and Tester, 1997) at the onset of the HAB of $\sim 10 \mu\text{g chl l}^{-1}$ that year (Fig. 3). On 5 August 1992, the WFS diet of *T. stylifera* was 18% microzooplankton, 62% nanoplankton, and 20% mainly toxic dinoflagellates (Kleppel et al., 1996). Farther upstream on the Louisiana shelf, based upon fecal pellet contents, the *C. velificatus* populations were raptorial (Tisellius, 1989) carnivores, while *T. turbinata* and *T. stylifera* were mainly herbivores (Turner, 1984; 1987), next to eutrophic nutrient supplies of the diatom-rich, Mississippi River plume (Dortch and Whittlestone, 1992).

Farther downstream on the more oligotrophic Georgia shelf of the South Atlantic Bight [SAB], based instead upon laboratory feeding experiments, both *C. velificatus* and *T. stylifera* were omnivores, when offered a selection of *Rhizosolenia* and copepod nauplii (Paffenhofer and Knowles, 1980). Additionally, half-saturation constants k_s for growth (Table 1) of either *C. typicus*, or *Acartia tonsa*, were $\sim 8 \mu\text{mol C l}^{-1}$ (Dagg and Grill, 1980; Mayzaud et al., 1998), such that at no time of the year did the mean WFS diatom stocks (Saunders and Glenn, 1969) of $\sim 3.3 \mu\text{mol C l}^{-1}$ biomass during 1947-1972 (Table 2) then amount to sufficient amounts of food for these facultative copepod omnivores, i.e. providing about 29% of their maximal ingestion demands via herbivory.

By 1986 within very far, upstream teleconnected waters (Walsh et al., 2011) of the Caribbean Sea, where similar overfishing off Jamaica had also occurred (Hughes, 1994), a ten-fold reduced seasonal maximum of only 3,930 ciliates l^{-1} was found off Kingston, Jamaica from other bottle samples in August-September 1986 (Lynn et al., 1991). With transit times of < 75 days for physical exchanges (Walsh et al., 2011) of both ciliate and tunicate microzooplankton populations within western boundary currents of the southern GOM, these upstream data provided inter-annual temporal sequences, despite spatial separation. The same protozoan carbon content

yielded an inferred post-cascade biomass estimate of $\sim 5.5 \mu\text{mol C l}^{-1}$ of ciliates during ~ 2001 - 2002 on the WFS (Table 2). Accordingly, ten-fold smaller boundary conditions of ciliates at the 5-m and 45-m isobaths were imposed in the models cases of 2001-2002 and 2010-2011 (Tables 4-5), compared to those of 1965-1966 (Table 3).

3.4.2 Tunicates

The model persistently overestimated the observed stocks of omnivore tunicates on the 20-m isobath during 1965-1966 (Fig. 9a), with then simulated underestimates of the “known” ciliate biomasses (Fig. 9b), like the inverse pools of ammonium and nitrate (Fig. 4). Herbivore competitors, i.e. meroplanktonic larval herbivore polychaetes (Table 2), had not been included as other state variables of the model to remove joint prey of the tunicates, thus initiating food limitation of these gelatinous predators in the “real world” (Hopkins, 1977; Badylak and Phlips, 2008). When oil-contamination was found on the WFS during 2010 (Weisberg et al., 2014a; McDaniel et al., 2015), with presumably greater impacts on tunicates (Nour El-Din and Al-Kayat, 2001) than ciliates (Andrews and Floodgate, 1974; Rogerson and Berger, 1981; Dale, 1987), greater fidelity of model results instead occurred (Fig. 9c). After oil spills, the observed tunicate stocks at the 5-m isobath then declined from 2001 to 2011 (Tables 4-5).

Without future correct assessments of natural mortalities of the tunicates, additional misunderstandings of plankton trophodynamics of coastal seas will continue, since the model also did not include additional food supplies of the tunicates. In laboratory analogues of the “real world”, *O. dioica* ate the prymnesiophyte microflagellates *I. galbana*, and diatoms, as well as ciliates *Strombidium* spp. (Lombard et al., 2013), similar to the diets of other omnivores, i.e. the copepods *C. typicus* (Wiadnyana and Rassoulzadegan, 1989). Field studies of predator-prey interactions within eutrophic ecosystems of the Baltic Sea, the English Channel, the Bay of Biscay, and the northern Chile upwelling system (Lopez-Urrutia et al., 2004; Vargas and Gonzalez, 2004; Tonnesson and Tisellius, 2005) also found that only 24% of the food of *O. dioica* was of micro-algal origin, with suggestions of their additional ingestion of ciliates.

For example, within Kiel Fjord, the chain-forming diatoms of the April-June 2001 spring blooms had a del N-15 of $+6.5\text{\textperthousand}$, while the del N-15 signatures of herbivorous *Pseudocalanus*, *Temora*, and bivalve veliger larvae were a mean of $8.9\text{\textperthousand}$ (Sommer and Sommer, 2004), yielding a trophic enrichment of $+2.4\text{\textperthousand}$. Yet, the del N-15 of *O. dioica* was then $+10.3\text{\textperthousand}$ (Sommer and

Sommer, 2004), thus feeding at a higher carnivore trophic level on presumably animal sources of protein, e.g. ciliates.

Accordingly, one second “cure” for the mismatches of our present model results with the microzooplankton observations (Fig. 9) would have been to instead feed more of the tunicates to simulated calanoid copepod omnivores, specifically their eggs of >40 microns size (Sommer et al., 2003; Lopez-Urrutia et al., 2004; Stibor et al., 2004) in an expanded set of life history state variables, before the oil spills. Recall that the first “cure” for the mismatched ammonium accumulation rates (Fig. 4) would have been use of a smaller rate of nitrification. Future numerical studies could accordingly include other case studies of greater ecological complexity, in which the ciliates would be the additional prey of oil-sensitive tunicate predators, with the potential to accelerate fallout of petrochemicals (Walsh et al., 2015a) and other pollutants to the sea floor (Allredge, 1976; Bruland and Silver, 1981; Lombard et al., 2010, 2013), while oxidation rates of ammonium were less within explicit 3-D descriptions of nitrate influxes from slope waters.

These tunicates shed houses at rates of 2-20 houses day⁻¹ (Sato et al., 2003), with sinking rates of 45-231 m day⁻¹, depending upon the ingested “ballast” within their houses (Lombard et al., 2013). Of course, if most of the tunicates were routinely eaten by *Centropages* and *Acartia* spp. (Sommer et al., 2003), major particle exits in the forms of either shed tunicate houses, or their extruded fecal pellets, would be moot. Instead, more phytoplankton toxins in aerosol stages would be left behind to exit global sea surfaces of HAB-ridden shelves (Walsh et al., 2015a, b).

Note that ~50.0 nmol C l⁻¹ of *T. turbinata* was observed and simulated on the 20-m isobath of the WFS in mid-January 2001 (Fig. 10c), before the *Deepwater Horizon* oil spills. Instead, a ~75% biomass reduction to ~12.0 nmol C l⁻¹ of these copepods occurred afterwards by January 2010, as again mimicked by the model (Fig. 10e). The observed stocks of *O. dioica* had similarly declined by 75%, from ~25.0 nmol C l⁻¹ on the 20-m isobath of the WFS in mid-January 2001 (Fig. 9c) to ~6.0 nmol C l⁻¹ of these tunicates by January 2010 (Fig. 9e).

These simulation results and data constraints suggested that: (1) compared to the oil-hardy ciliates, the calanoid copepod omnivores may have been equally sensitive to petroleum poisons as their competing tunicate omnivores; (2) significant oil loadings from the *Deepwater Horizon* blowout (Fig. 1) must have indeed penetrated the inner WFS (Weisberg et al., 2015a; McDaniel et al., 2015) to reduce the observed stocks of both *T. turbinata* and *O. dioica*, by as much as 75% up

to January 2010, approximated by the 2-D model predictions (Figs. 9c, e; 10c, e); and (3) a combination of both trophic cascades and oil spills were required for persistent, but perhaps not irrevocable, alterations of marine system states, with consequent public health maladies among downwind adjacent human populations.

3.5 Mesozooplankton

As a result of past overfishing, mercury releases, pesticide poisonings, and now a ~30-year history of oil platform blowouts on both sides of the GOM, regional zooplankton herbivores had declined ~10-fold, based upon sampling of GOM copepod populations, with plankton nets of varying mesh sizes up to 333 microns, from 1949 to 2011 (Walsh et al., 2015a). Here, we compiled another time series of shorter interval, from 1965 to 2002, based on additional samples from the WFS, obtained instead by bottle and pump casts of zooplankton larval stages. These additional data were corroborated by the net samples of adult abundances. But, the larval zooplankton stages were collected with more efficient 41-74 microns (Hopkins, 1977; Badylak and Phlips, 2008) and 145-153 microns (King, 1950; Lester et al., 2008) mesh sizes, until the nets clogged. The larger mesh size nets undersampled the juvenile phases of copepods, caught instead with smaller 64 microns mesh nets (Baier and Purcell, 1997).

A seasonal maximal copepod larval population of 3725 nauplii l^{-1} was counted by Karen Steidinger along the 5-m isobath of the WFS (Fig. 1) in August-September 1965, using bottle samples (Joyce and Williams, 1969) during a small HAB of $\sim 1.5 \mu g chl l^{-1}$ (1.5×10^5 cells l^{-1}) in October 1965 (Fig. 3). About 40 years later during August-September 2002, only 225 nauplii l^{-1} were observed at the ~5-m isobath near the mouth of Tampa Bay (Fig.1), using again water samples, rather than nets (Badylak and Phlips, 2008). Then, about $2 \mu g l^{-1}$ of total bulk chlorophyll occurred there (Badylak and Phlips, 2008) during a similar small red tide of $\sim 1 \mu g chl l^{-1}$ (1×10^5 cells l^{-1}) in October 2002 (Fig. 3), such that altered amounts of HAB poisoners over time were presumably not a factor in the ten-fold decline of seasonal WFS abundances of copepod nauplii.

These early life history stages of copepods had a carbon biomass of nauplii = stage 1 copepodites (Mauchline, 1998) for both *C. velificatus* and *T. turbinata* of ~ 2.5 nmol C per each individual (Chisholm and Roff, 1990), where C = 32% dw (Wiebe et al., 1975). Thus, a maximum early life history abundance of ~ 3725 nauplii l^{-1} amounted to $\sim 0.9 \mu mol C l^{-1}$ of nauplii during August-September 1965. These newly hatched copepodite omnivores would have eventually eaten

phytoplankton, ciliates, tunicates, and other copepod herbivores over their life histories of a few months duration. In turn, they served as prey of the competing larval fish, chaetognath, and scyphomedusa predators in pre-cascade and post-cascade carbon budgets here of changing plankton pyramids of biomass on the WFS (Table 2).

Accordingly, in the first carbon budget of the pre-cascade plankton state (Table 2), the seasonal naupliar maximum along the WFS 5-m isobath during August-September 1965 of initial larval copepod stages was assumed to be still dominated (King, 1950) by the omnivores *Centropages* and *Acartia*. Away from estuarine areas, adult female stocks of *Centropages* spp. on the WFS (Lester et al., 2008) also had to have been present during the preceding 10.8 hours at $\sim 25^{\circ}\text{C}$ (Joyce and Williams, 1969), based on a mean naupliar duration stage of 32.3 hours at 15°C and a Q_{10} (Table 1) of 3.0 (Huntley and Lopez, 1992; Kiorboe and Sabatini, 1995). Since *C. velificatus* and *T. turbinata* had similar sizes and growth rates of $0.5\text{-}0.6\text{ day}^{-1}$ (Table 1) at $\sim 30^{\circ}\text{C}$ (Chisholm and Roff, 1990), with the same temperature Q_{10} for these copepods of 3.0 (Huntley and Lopez, 1992), the physiological parameters of the former copepod were used to estimate trophic exchanges among different biomasses of WFS plankton omnivores during 1948-1972 and 2001-2002 (Table 2).

Eggs of the broadcast spawning *Centropages* spp. of the WFS were further assumed to have a mean weight of $2.8\text{ nmol C egg}^{-1}$, produced by females of a larger mean weight of $1.0\text{ }\mu\text{mol C individual}^{-1}$. Their mean egg production rate may have been $63\text{ eggs female}^{-1}\text{ day}^{-1}$, or $\sim 29\text{ eggs female}^{-1}$ over the same 11 hours of naupliar maturation (Corkett and Zillioux, 1975; Dagg, 1978; Klein Breteler et al., 1982; Smith and Lane, 1985; Nival et al., 1990; Fryd et al., 1991; Davis and Alatalo, 1992).

Finally, given a 3% mortality of copepod eggs over the first 11 hours of post-hatch survival (Hirst and Kiorboe, 2002), an equivalent number of $\sim 350\text{ eggs l}^{-1}$ would have led to the observed $0.9\text{ }\mu\text{mol C l}^{-1}$ of nauplii in 1965. With such an egg production rate, 12 females l^{-1} would have amounted to an adult spawning population of $12.5\text{ }\mu\text{mol C l}^{-1}$ of copepods during 1965. A sex ratio of 2 females for every one male copepod (Hirst and Kiorboe, 2002) suggested a total pre-cascade adult population then of perhaps $18.3\text{ }\mu\text{mol C l}^{-1}$ of total copepod omnivores (Table 2) on the nearshore WFS in August 1965.

About two decades earlier, before onset of the trophic cascade, the seasonal maximum of measured zooplankton biomasses between the 4-m and 9-m isobaths off Charlotte Harbor had been a larger displacement volume of 44 ml m^{-3} (King, 1950), or perhaps $\sim 70.4 \text{ } \mu\text{mol C l}^{-1}$ (Khromov, 1969; Wiebe et al., 1975) in August 1949. At that time, the copepods *Centropages*, *Acartia*, and *Temora* spp., as well as the ciliates *Euplotes* spp., were again the dominant omnivores (King, 1950), presumably exerting top-down controls of the subsequent small HABs found during 1957-1959 (Fig. 3).

3.6 Carbon budgets

3.6.1 Pre-cascade

Overfishing of the piscivore red snapper *L. campechanus* after 1965 (Porch et al., 2007) had initiated a trophic cascade on the WFS (Walsh et al., 2011). At that time, estimated non-toxic carbon biomasses (Table 2) were $75.8 \text{ } \mu\text{mol C l}^{-1}$ of dinoflagellates, e.g. *Peridinium* spp. found both on the WFS (Steidinger and Williams, 1970) and off Veracruz (Garate-Lizarraga and Muneton-Gomez, 2008), and of $3.3 \text{ } \mu\text{mol C l}^{-1}$ of diatoms before Si-limitation, e.g. *Rhizosolenia* (Saunders and Glenn, 1969). Together, they may have contributed a combined pre-cascade phytoplankton sum of $79.1 \text{ } \mu\text{mol C l}^{-1}$ to the edible prey fields of *C. velificatus* on the WFS. The estimated pre-cascade carbon biomass of $\sim 0.3 \text{ } \mu\text{mol C l}^{-1}$ of small microflagellates, e.g. *I. galbana*, would not have been directly available to copepod omnivores (Paffenhofer, 1984; Fulton, 1984), without 90% respiration losses via ciliate and tunicate microzooplankton transfers. But, they were still included here as realized “known” biomasses of the protozoans and metazoans (Tables 2-5).

Such a sum then of $66.8 \text{ } \mu\text{mol C l}^{-1}$ of microzooplankton ciliates and tunicates could have provided more of the food menu of these crustacean omnivores during 1948-1973 (Table 4). We used the 10% transfer efficiency between omnivore copepods and their algal and animal prey fields confirmed here in the model results (Table 6). Accordingly, this trophic pyramid at the 5-m isobath required a total pre-cascade food source of $183.0 \text{ } \mu\text{mol C l}^{-1}$ for those copepod omnivores, of which $145.9 \text{ } \mu\text{mol C l}^{-1}$, or $\sim 80\%$, could have been supported by the stocks of presumed edible phytoplankton and microzooplankton during 1947-1972 (Table 4). What were the other food supplies?

Along the 5-m isobath at the mouth of Tampa Bay, the pre-cascade micrometazoan populations of mainly bivalve and polychaete larvae were the dominant meroplankton components

(Hopkins, 1977). They represented potential seasonal planktonic food for WFS copepod omnivores, like the prey of *Acartia bifilosa* and *A. clausi* found in European estuaries (Sautour and Castel, 1995). Laboratory populations of the meroplanktonic larvae of both mussels *Mytilus edulis* (Fotel et al., 1999) and polychaetes *Mediomastus fragile* (Hansen, 1993) also readily ate the microflagellates *I. galbana*. Decadal increments (Badylak and Philips, 2008) of these WFS summer maximal larval herbivore populations thus started from a baseline in lower Tampa Bay of 17.6 veliger larvae l^{-1} of bivalves and of 3.4 polychaete larvae l^{-1} of annelid worms during August 1970 (Hopkins, 1997).

The field abundances of the dominant meroplankton larvae had respective carbon contents of 0.4 $\mu\text{g C individual}^{-1}$ for bivalves (Fotel et al., 1999) and 0.2 $\mu\text{g C worm}^{-1}$ for polychaetes (Hansen, 1993). So, their initial pre-cascade stocks amounted to combined larval invertebrate food sources for the copepod omnivores of 7.7 $\mu\text{mol C l}^{-1}$ in 1970, i.e. another 4% of the first carbon budget during 1947-1973 (Table 2). Thus far, all of these potential prey organisms had yielded a cumulative sum of 84% of the estimated food demands of pre-cascade copepod omnivores.

Depending upon the realized palatability of *K. brevis* to copepods (Gill and Harris, 1987; Uye and Takamatsu, 1990; Turner and Tester, 1997; Speckmann et al., 2006; Cohen et al., 2007; Breier and Buskey, 2007; Waggett et al., 2012; Turner et al., 2012; Lauritano et al., 2013), all of the small amount of pre-cascade HABs of 12.5 $\mu\text{mol C l}^{-1}$ may have then been eaten by the copepod omnivores. In this scenario, a penultimate 7% of the annual carbon demands of such copepods could have been met by HABs, with perhaps 9% left still “*unknown*”, in the absence of invocation of larger trophic transfer efficiencies. Indeed, if the copepod omnivores had not removed most of the pre-cascade secondary production of these HABs, despite their inadequate nutrition, relaxation of grazing pressures would not have led to the much larger subsequent post-cascade HABs on the WFS (Fig. 3).

Other consideration of more energy transfers to predators at the next higher trophic level, with the same ecological efficiency of 10%, would have required a WFS predator stock of 1.83 $\mu\text{mol C l}^{-1}$ of vertebrate and invertebrate zooplanktivores in the pre-cascade trophic pyramid of 1948-1973 (Table 2). Within GOM and SAB waters, a combined biomass sum of ~0.84 $\mu\text{mol C l}^{-1}$ of larval fish (Houde and Chitty, 1976), chaetognath (Pierce, 1951; Reeve, 1964; Mulkana and McIlwain, 1973), and scyphomedusa (Burke, 1975) predators was estimated at this trophic level

in the first carbon budget (Table 2). In the next post-cascade budget, a jellyfish predator biomass of $\sim 0.02 \mu\text{mol C l}^{-1}$ was instead again inferred from a 10% ecological efficiency of element transfers, compared to $\sim 0.03 \mu\text{mol C l}^{-1}$ obtained from additional independent estimates (Graham, 2002) of separate summer biomasses of these carnivores over 2001-2010 (Table 2).

3.6.2 Post-cascade

Using a similar mesh size in the same area of the WFS, a ten-fold smaller amount of 225 total copepod nauplii l^{-1} was found near the 5-m isobath at the mouth of Tampa Bay in August-September 2002 (Badylak and Phlips, 2008). These observations yielded a post-cascade adult omnivore stock of just $1.1 \mu\text{mol C l}^{-1}$ (Table 2), based upon the same assumptions and conversion factors (Table 1). Then, their ingestion demands of $11.0 \mu\text{mol C l}^{-1}$ could have been easily met by the combined potential prey sum of $145.6 \mu\text{mol C l}^{-1}$, derived from: $2.3 \mu\text{mol C l}^{-1}$ of tunicates; $5.5 \mu\text{mol C l}^{-1}$ of ciliates; $8.8 \mu\text{mol C l}^{-1}$ of diatoms; and $129.0 \mu\text{mol C l}^{-1}$ of meroplanktonic larvae, without additional utilization at that time of the ungrazed HABs (Table 4), which had replaced the peridinians (Steidinger and Williams, 1970) as the dominant dinoflagellates.

The observed meroplanktonic increments to ~ 315 veliger larvae l^{-1} and ~ 15 polychaete larvae l^{-1} in June 2002 (Badylak and Phlips, 2008) summed to an equivalent biomass of $\sim 129 \mu\text{mol C l}^{-1}$ in the second post-cascade budget over 2001-2002. Such biomass increases reflected the >10 -fold smaller amount of their post-cascade copepod predators (Table 2). Corroboration of these observations was provided by an earlier zooplankton time series (Walsh et al., 2011), employing different, but consistent sampling techniques. Along the 5-10 m isobaths of the WFS during August 1973, bongo nets of 333 microns mesh size caught a mean displacement volume of $\sim 0.30 \text{ ml total adult zooplankton m}^{-3}$ over 20 nearshore stations (Houde and Chitty, 1976). With the same type of nets and mesh sizes over a similar station grid two decades later, the WFS total zooplankton biomass had declined to $\sim 0.03 \text{ ml m}^{-3}$ by August 1993 (Walsh et al., 2011).

Finally, recall that the regional GOM satellite observations and *in situ* algal cell counts (Fig. 3) of increased phytoplankton biomass confirmed the apparent inverse declines of zooplankton biomass on both sides of the GOM (Walsh et al., 2015a), as well as in other coastal isomorphs of another 24 zooplankton time series (Walsh et al. 2015b). It was unlikely that increased temperatures of global warmings and associated coral bleachings had led to decreases in gross zooplankton growth rates (Banse, 1982; Huntley and Lopez, 1992). So, the most feasible

long-term scenarios for these zooplankton and phytoplankton observations at regional GOM and global scales involved world-wide marine trophic cascades (Paine, 1980; Carpenter et al., 1985; Pauly et al., 1998; Pace et al., 1999; Frank et al., 2005; Walsh et al., 2011), with increased fatal pulmonary consequences for adjacent humans, including perhaps ~13% of the ~2 million children of <5 years of age, who died from pneumonia during 2004 (Wardlaw et al., 2006).

4. DISCUSSION

Given a reduction of copepod facultative herbivore biomasses of $17.2 \text{ umol C l}^{-1}$ between 1965-1966 and 2001-2002 (Fig. 10) and a 10% ecological transfer efficiency (Table 2), the no longer consumed algal prey would have amounted to an ungrazed increment of $172.0 \text{ umol C l}^{-1}$ of all phytoplankton over the same time period. Then, the respective increases of particulate stocks of microflagellates were negligible, whereas the sum of particulate HAB and diatom population increments [$112.5 + 5.5 \text{ umol C l}^{-1}$] was $118.0 \text{ umol C l}^{-1}$ (Table 2). This difference of 54 umol C l^{-1} presumably represented export of bacterial-lysed HAB cells in dissolved form, with subsequent expulsions from surface sea waters each year as HAB aerosols within wind-borne sea spray (Walsh et al., 2015a).

Such an inferred NE Gulf of Mexico aerosol flux amounted here to 48% of the net total carbon sequestration by HABs on the WFS between 1965-1966 and 2001-2002, i.e. $54.0 \text{ umol C l}^{-1}$ of the decadal increment of $112.5 \text{ umol C l}^{-1}$ (Table 2). It was traced downstream later in 2007 as known county-wide asthma hospitalization rates over the southeastern United States (Walsh et al., 2015a). Globally the landward dispersion of marine HAB asthma triggers caused about 13% of the world-wide malign pulmonary events, i.e. ~40 million asthma attacks, among adjacent humans during 2004 (Walsh et al., 2015b). Given now a quantitative definition of the magnitude of these marine poison impacts from regional and global seas, future construction of operational forecasts models next becomes a feasible, societally-relevant goal, analogous to routine ongoing forecasts of storm surges, for proactive prediction and alleviation of pulmonary disease consequences among both developing and developed sea-side nations.

Acknowledgements

This research was made possible in part by a grant from The Gulf of Mexico Research Initiative, and in part by NOAA grant NA15NOS4780174 to RHW, JJW, and JML. Our Collaboration for Prediction of Red tide (CPR) project also received support from the Florida Fish and Wildlife

Research Institute (FWRI). Data are publicly available through the Gulf of Mexico Research Initiative Information & Data Cooperative (GRIIDC) at <https://data.gulfresearchinitiative.org> (UDI: [R4.x267.182:0002](#)). We'd also thank Drs. Karen Steidinger, Alina Corcoran and Kendra Daly for use of their data. This is CPR contribution #38.

References

Acuna, J.L. and M. Kiefer. 2000. Functional response of the appendicularian *Oikopleura dioica*. Limnol. Ocean. 45, 606-618.

Adams, D.H., and R.H. McMichael. 2007. Mercury in king mackerel, *Scomberomorus cavalla*, and Spanish mackerel, *S. maculatus*, from waters of the southeastern USA: Regional and historical trends. Mar. Freshwat. Res. 58, 187-193.

Alldredge, A.L. 1976. Discarded appendicularian houses as sources of food, surface habitats, and particulate organic matter in planktonic environments. Limnol. Oceanogr. 21, 14-23.

Andrews, A.R. and G.D. Floodgate. 1974. Some observations on the interactions of marine protozoa and crude oil residues. Mar. Biol. 25, 7-12.

Azam, F. and R.E. Hudson. 1981. Multiphase kinetics for d-glucose uptake by assemblages of natural marine bacteria. Mar. Ecol. Prog. Ser. 6, 213-222.

Azam, F. and F. Malfatti. 2007. Microbial structuring of marine ecosystems. Nat. Rev. Mirob. 5, 782-791.

Baden, D.G., and T.J. Mende. 1982. Toxicity of two toxins from the Florida red tide dinoflagellate, *Ptychodiscus brevis*. Toxicon 20, 457-461.

Badylak, S. and E.J. Phlips. 2008. Spatial and temporal distributions of zooplankton in Tampa Bay, including observations during a HAB event. J. Plank. Res. 30, 449-465.

Baier, C.T. and J.E. Purcell. 1997. Trophic interactions of chaetognaths, larval fish, and zooplankton in the South Atlantic Bight. Mar. Ecol. Prog. Ser. 146, 43-53.

Banse, K. 1982. Rates of growth, respiration, and photosynthesis of unicellular algae and ciliates, the role of ciliates in the marine pelagic. Limnol. Oceanogr. 13, 135-140.

Bernard, C. and F. Rassoulzadegan. 1990. Bacteria or microflagellates as a major food source for marine ciliates: Possible implications for the microzooplankton. Mar. Ecol. Prog. Ser. 64, 147-155.

Bianchi, M., P. Bonin, and Feliatra. 1994. Bacterial nitrification and denitrification in the Rhone River plume (northwestern Mediterranean Sea). Mar. Ecol. Progr. Ser. 103, 197-201.

Bianchi, M., Feliatra, and D. Lefevre. 1999. Regulation of nitrification in the land-ocean contact area of the Rhone River plume (NW Mediterranean). Aquat. Microbiol. Ecol. 18, 301-312.

Bledsoe, E. and E.J. Phlips. 2000. Relationships between phytoplankton standing cop and physical, chemical and biological gradients in the Suwannee River and plume region, U.S.A. Estuaries 23, 458-473.

Breier, C.F. and E.J. Buskey. 2007. Effects of the red tide dinoflagellate *Karenia brevis* on grazing and fecundity in the copepod *Acartia tonsa*. J. Plankt. Res. 29, 116-126.

Bruland, K.W. and M.W. Silver. 1981. Sinking rates of fecal pellets from gelatinous zooplankton (salps, pteropods, doliolids). Mar. Biol. 63, 295-300.

Burke, W.D. 1975. Biology and distribution of the macrocoelenterates of Mississippi Sound and adjacent waters. Gulf Res. Rep. 5, 17-22.

Burkhardt, S., I. Zondervan, and U. Riebesell. 1999. Effects of CO₂ enrichment on C:N:P ratio in marine phytoplankton: A species comparison. Limnol. Oceanogr. 44, 683-690.

Burns, B.D. and J. Beardall. 1987. Utilization of inorganic carbon by marine microalgae. J. Exp. Mar. Biol. Ecol. 107, 75-86.

Button, D.K., B.R. Robertson, D. McIntosh, and F. Juttner. 1992. Interactions between marine bacteria and dissolved-phase and beached hydrocarbons after the *Exxon Valdez* oil spill. *Appl. Environ. Microbiol.* 58, 243-251.

Caperon, J. and D.F. Smith. 1978. Photosynthetic rates of marine algae as a function of inorganic carbon concentration. *Limnol. Oceanogr.* 23, 704-708.

Carls, M.G. and S.D. Rice. 1989. Abnormal development and growth reductions of pollock *Theragra chalcogramma* embryos exposed to water-soluble fractions of oil. *Fish. Bull.* 88, 29-37.

Carpenter, E.J. and T. Roenneberg. 1995. The marine planktonic cyanobacterium *Trichodesmium* spp.: Photosynthetic rate measurements in the SW Atlantic Ocean. *Mar. Ecol. Progr. Ser.* 118, 267-273.

Carpenter, S.R., J.F. Kitchell, and J.R. Hodgson. 1985. Cascading trophic interactions and lake productivity: Fish predation and herbivory can regulate lake ecosystems. *Bioscience* 35, 634-639.

Cherrier, J., J.E. Bauer, E.R. Druffel, R.B. Coffin, and J.P. Chanton. 1999. Radiocarbon in marine bacteria: Evidence for the ages of assimilated carbon. *Limnol. Oceanogr.* 44, 730-736.

Chisholm, L.A. and J.C. Roff. 1990. Size-weight relationships and biomass of tropical neritic copepods off Kingston, Jamaica. *Mar. Biol.* 106, 71-77.

Choi, S.-C. and R. Bartha. 1994. Environmental factors affecting mercury methylation in estuarine sediments. *Bull. Environ. Contam. Toxicol.* 53, 805-812.

Coachman, L. K., and J. J. Walsh. 1981. A diffusion model of cross-shelf exchange of nutrients in the Bering Sea. *Deep-Sea Res.* 28:819-837.

Cohen, J.H., P.A. Tester, and R.B. Forward. 2007. Sublethal effects of the toxic dinoflagellate *Karenia brevis* on marine copepod behavior. *J. Plank. Res.* 29, 301-315.

Collins, L.A., G.R. Fitzhugh, L. Mourand, L.A. Lombardi, W.T. Walling, W.A. Fable, M.R. Burnett and R.J. Allman. 2001. Preliminary results from a continuing study of spawning and fecundity in the red snapper (Lutjanidae: *Lutjanus campechanus*) from the Gulf of Mexico. *Proc. Gulf Carrib. Fish. Inst.* 52, 34-47.

Compeau, G.C. and R. Bartha. 1985. Sulfate-reducing bacteria: Principal methylators of mercury in anoxic estuarine sediments. *App. Environ. Microbiol.* 50, 498-502.

Corkett, C.J. and F.J. Zillioux. 1975. Studies on the effect of temperature on the egg laying of three species of calanoid copepods in the laboratory (*Acartia tonsa*, *Temora longicornis*, and *Pseudocalanus elongatus*). *Bull. Plank. Soc. Jap.* 21, 13-21.

Coston-Clements, L., R.J. Waggett, and P.A. Tester. 2009. Chaetognaths of the United States South Atlantic Bight: Distribution, abundance and potential interactions with newly spawned larval fish. *J. Exp. Mar. Biol. Ecol.* 373, 111-123.

Craig, J.M., P.L. Klerks, K. Heimann, and J.L. Waits. 2003. Effects of salinity, pH and temperature on the re-establishment of bioluminescence and copper, or SDS toxicity, in the marine dinoflagellate *Pyrocystis lunula* using bioluminescence as an endpoint. *Environmental Pollution* 125:267-375.

Dagg, M.J. 1978. Estimated *in situ* rates of egg production for the copepod *Centropages typicus* (Kroyer) in the New York Bight. *J. Exp. Mar. Biol. Ecol.* 34, 183-196.

Dagg, M.J. and J.J. Govoni. 1996. Is ichthyoplankton predation an important source of copepod mortality in subtropical coastal waters? *Mar. Freshwater Res.* 47, 137-144.

Dagg, M.J. and D.W. Grill. 1980. Natural feeding rates of *Centropages typicus* females in the New York Bight. *Limnol. Oceanogr.* 25, 597-609.

Dale, T. 1987. Oil pollution and plankton dynamics. II. Abundance pattern of ciliates inside and outside enclosures and the responses of ciliates to oil during the 1980 spring bloom in Lindaspollene, Noway. *Sarsia* 72, 197-202.

Darrow, B.P., J.J. Walsh, G.A. Vargo, R.T. Masserini, K.A. Fanning, and J.-Z. Zhang. 2003. A simulation study of the growth of benthic microalgae following the decline of a surface phytoplankton bloom. *Cont. Shelf Res.* 23, 1265-1283.

Davis, C.O., N.F. Breitner, and P.J. Harrison. 1978. Continuous culture of marine diatoms under silicon limitation. III. A model of Si-limited diatom growth. *Limnol. Oceanogr.* 23, 41-52.

Davis, C.S. and P. Alatalo. 1992. Effects of constant and intermittent food supply on life-history parameters in a marine copepod. *Limnol. Oceanogr.* 37, 1618-1639.

Deveraux, R., M.R. Winfrey, J. Winfrey, D.A. Stahl. 1996. Depth profile of sulfate-reducing bacterial ribosomal RNA and mercury methylation in an estuarine sediment. *FEMS Microbiol. Ecol.* 20, 23-31.

Di Capua, I. and M.G. Mazzocchi. 2004. Population structure of the copepods *Centropages typicus* and *Temora stylifera* in different environmental conditions. *ICES J. Mar. Sci.* 632-644.

Dolan, D.M., V.J. Bierman, M.H. Dipert, and R.D. Geist. 1978. Statistical analysis of the spatial and temporal variability of the ratio chlorophyll *a* to phytoplankton cell volume in Saginaw Bay, Lake Huron. *Int. Assoc. Great Lakes Res.* 4, 75-83.

Dortch, Q. and T.E. Whitledge. 1992. Does nitrogen or silicon limit phytoplankton production in the Mississippi River plume and nearby regions? *Cont. Shelf Res.* 12, 1293-1309.

Eppley, R.W., J.N. Rogers, and J.J. McCarthy. 1969. Half-saturation constants for uptake of nitrate and ammonium by marine phytoplankton. *Limnol. Oceanogr.* 14, 912-920.

Fagerbakke, M. Heldal, and S. Norland. 1996. Content of carbon, nitrogen, oxygen, sulphur, and phosphorus in native aquatic and cultured bacteria. *Aquat. Microb. Ecol.* 10, 15-27.

Falkowski, P.G., T.S. Hopkins, and J.J. Walsh. 1980. An analysis of factors affecting oxygen depletion in the New York Bight. *J. Mar. Res.* 38:479-506.

Fath, B.D. and B.C. Patten. 1998. Network synergism: Emergence of positive relations in ecological systems. *Ecol. Mod.* 107, 127-143.

Fenchel, T. and P.R. Jonsson. 1988. The functional biology of *Strombidium sulcatum*, a marine oligotrich ciliate (Ciliophora, Oligotrichina). *Mar. Ecol. Progr. Ser.* 48, 1-15.

Fotel, F.L., N.J. Jensen, L. Wittrup, and B.W. Hansen. 1999. *In situ* and laboratory growth by a population of blue mussel larvae (*Mytilus edulis* L.) from a Danish embayment, Knebel Vig. *J. Exp. Mar. Biol. Ecol.* 233, 312-230.

Frank, K.T., B. Petrie, J.S. Choi, and W.C. Leggett. 2005. Trophic cascades in a formerly cod-dominated ecosystem. *Science* 308, 1621-1623.

Fryd, M., O.H. Haslund, and O. Wohlgemuth 1991. Development, growth, and egg production of two copepod species *Centropages hamatus* and *Centropages typicus* in the laboratory. *J. Plank. Res.* 13, 683-689.

Fukuda, R., H. Ogawa, T. Nagta, and I. Koike. 1998. Direct determination of carbon and nitrogen contents of natural bacterial assemblages in marine environments. *Appl. Environ. Microbiol.* 64, 3352-3358.

Fulton, R.S. 1984. Predation, production, and the organization of an estuarine zooplankton community. *J. Plankt. Res.* 6, 399-415.

Furnas, M.J. 1991. Net *in situ* growth rates of phytoplankton in an oligotrophic, tropical shelf ecosystem. *Limnol. Oceanogr.* 36, 13-29.

Gardner, W.S., R. Benner, R.M. Amon, J.B. Cotner, J.F. Cavaletto, and J.R. Johnson. 1996. Effects of high-molecular-weight dissolved organic matter on nitrogen dynamics in the Mississippi River plume. *Mar. Ecol. Progr. Ser.* 133, 287-297.

Garate-Lizarraga, I. and M.S. Muneton-Gomez. 2008. Bloom of *Peridinium quinquecorne* Abe in La Ensenada de La Paz, Gulf of California (July 2003). *Acta Bot. Mex.* 83, 33-47.

Gifford, D.J. and M.J. Dagg. 1988. Feeding of the estuarine copepod *Acartia tonsa* Dana: Carnivory vs. herbivory in natural microplankton assemblages. *Bull. Mar. Sci.* 43, 458-468.

Gill, C.W. and R.P. Harris. 1987. Behavioural responses of the copepods *Calanus helgolandicus* and *Temora longicornis* to dinoflagellate diets. *J. Mar. Biol. Ass. U.K.* 67, 785-801.

Goldman, J.C. and M.R. Dennett. 2000. Growth of marine bacteria in batch and continuous culture under carbon and nitrogen limitation. *Limnol. Oceanogr.* 45, 789-800.

Gorsky, G., I. Palazzoli, and R. Fenaux. 1987. Influence of temperature changes on oxygen uptake and ammonia and phosphate excretion in relation to body size and weight in *Oikopleura dioica* (Appendicularia). *Mar. Biol.* 94, 191-201.

Graham, W.M. 2001. Numerical increases and distributional shifts of *Chrysaora quinquecirrha* (Desor) and *Aurelia aurita* (Linne) (Cnidaria: Scyphozoa) in the northern Gulf of Mexico. *Hydrobiologia* 451, 97-111.

Graham, W.M. 2002. Carnivorous jellyfish. In *An ecosystem model of the West Florida shelf for use in fisheries management and ecological research: Volume II. Model construction*, eds. T.A. Okey and B. Mahmoudi, FL. Mar. Res. Inst., Fish Wildlife Conser. Comm., St. Petersburg, pp 45-46.

Guzman del Proo, S.A., E.A. Chavez, F.M. Altavriste, S. de la Campa, G. De la Cruz, L. Gomez, R. Guadarrama, A. Guerra, S. Mille, and D. Torruco. 1986. The impact of the IXTOC-1 oil spill on zooplankton. *J. Plank. Res.* 8, 557-581.

Halsband-Lenk, C., H.-J. Hirche, and F. Carlotti. 2002. Temperature impact on reproduction and development of congener copepod populations. *J. Exper. Mar. Biol. Ecol.* 271, 121-153.

Hansen, B. 1993. Aspects of feeding, growth, and stage development by trophophora larvae of the boreal polychaete *Mediomastus fragile* (Rasmussen) (Capitellidae). *J. Exp. Mar. Biol. Ecol.* 166, 273-288.

Hansson, L.J. 1997. Effect of temperature on growth rate of *Aurelia aurita* (Cnidaria, Scyphozoa) from Gullmarsfjorden, Sweden. *Mar. Ecol. Progr. Ser.* 161, 145-153.

Harrison, W.G., D. Douglas, P.G. Falkowski, G.T. Rowe, and J. Vidal. 1983. Summer nutrient dynamics of the Middle Atlantic Bight: Nitrogen uptake and regeneration. *J. Plank. Res.* 5, 539-556.

Hassett, R.P. and E.L. Crockett. 2009. Habitat temperature is an important determinant of cholesterol contents in copepods. *J. Exper. Biol.* 212, 71-77.

Heil, C.A., M.R. Mulholland, D.A. Bronk, P. Bernhardt, and J.M. O'Neil. 2004. Bacterial and size fractionated primary production within a large *Karenia brevis* bloom on the West Florida shelf. In *Harmful Algae 2002*, eds. K.A. Steidinger, J.H. Landsberg, C.R. Tomas, and G.A. Vargo, UNESCO, Paris, pp 38-40.

Heimann, K., J.M. Matuszewski, and P.L. Klerks. 2002. Effects of metals and organic contaminants on the recovery of bioluminescence in the marine dinoflagellate *Pyrocystis lunula* (Dinophyceae). *J. Phycol.* 38, 482-492.

Herzig, R. and P.G. Falkowski. 1989. Nitrogen limitation in *Isochrysis galbana* (Haptophyceae). I. Photosynthetic energy conversion and growth efficiencies. *J. Phycol.* 25, 462-471.

Hirst, A.G. and T. Kiorboe. 2002. Mortality of marine planktonic copepods: Global rates and patterns. *Mar. Ecol. Progr. Ser.* 230, 195-209.

Hobson, L.A., F.A. Hartley, and D.E. Ketcham. 1979. Effects of variations in daylight and temperature on net rates of photosynthesis, dark respiration and excretion by *Isochrysis galbana* Parke. *Plant Physiol.* 63, 947-951.

Hopcroft, R.R., J.C. Roff, and H.A. Bouman. 1998. Zooplankton growth rates: The larvaceans *Appendicularia*, *Fritillaria*, and *Oikopleura* in tropical waters. *J. Plank. Res.* 20, 539-555.

Hopkins, T.L. 1977. Zooplankton distribution in surface waters of Tampa Bay. *Bull. Mar. Sci.* 27, 467-478.

Houde, E.D. and N. Chitty. 1976. Seasonal abundance and distribution of zooplankton, fish eggs, and fish larvae in the eastern Gulf of Mexico, 1972-74. NOAA Tech. Rep. NMFS SSRF-701, Seattle WA, pp. 1-18.

Hu, C., R.H. Weisberg, Y. Liu, L. Zheng, K.L. Daly, D.C. English, Y. Zhao, and G.A. Vargo. 2011. Did the northeastern Gulf of Mexico become greener after the Deepwater Horizon oil spill? *Geophys. Res. Lett.* 38, L09061, doi:10.1029/2011GL047184.

Hughes, T.P. 1994. Catastrophes, phase shifts, and large-scale degradation of a Caribbean coral reef. *Science* 265, 1547-1551.

Hunt, D.E., L.A. David, D. Gevers, S.P. Preheim, E.J. Alm, and M.F. Polz. 2008. Resource partitioning and sympatric differentiation among closely related bacterioplankton. *Science* 320, 1081-1086.

Huntley, M.E. and M.D. Lopez. 1992. Temperature-dependent production of marine copepods: A global synthesis. *Amer. Nat.* 140, 201-242.

Jochens, A.E. and W.D. Nowlin. 2000. Northeastern Gulf of Mexico Chemical Oceanography and Hydrography Study, Annual Report. OCS Study MMS 2000-078, U.S. Dept. of the Interior, Minerals Management Service, Gulf of Mexico OCS Region, New Orleans, LA, pp. 1-89.

Jones, K.L., C.M. Mikulski, A. Barnhorst, and G.J. Doucette. 2010. Comparative analysis of bacterioplankton assemblages from *Karenia brevis* bloom and nonbloom water on the west Florida shelf (Gulf of Mexico, USA) using 16S rRNA gene clone libraries. *FEMS Microbiol. Ecol.* 73, 468-485.

Joyce, E.A. and J. Williams. 1969. Rationale and pertinent data. *Mem. Hourglass Cruises*, Vol. 1, Part I, pp 1-50.

Jurado, J.L., G.L. Hitchcock, and P.B. Ortner. 2007. Seasonal variability in nutrient and phytoplankton distributions on the southwestern Florida inner shelf. *Bull. Mar. Sci.* 80, 21-43.

Kannan, K., R.G. Smith, R.F. Lee, H.L. Windom, P.T. Heitmuller, J.M. Macauley, and J.K. Summers. 1997. Distribution of total mercury and methyl mercury in water, sediments, and fish from South Florida estuaries. *Archiv. Environ. Contam. Toxicol.* 34, 109-118.

Ketchum, B.H. and D.J. Keen. 1955. Accumulation of river water over the continental shelf between Cape Cod and Chesapeake Bay. *Deep-Sea Res.* 3, 346-357.

Khromov, N.S. 1969. Distribution of plankton in the Gulf of Mexico and some aspects of its seasonal dynamics. In *Soviet-Cuban Fishery Research*, editor A.S. Bogdanov, Israel Progr. Sci. Trans., Jerusalem, pp. 36-56.

Kim, D.I., Y. Matusyama, S. Nagasoe, M. Yamaguchi, Y.H. Yoon, Y. Ohima, N. Imada, and T. Honjo. 2004. Effects of temperature, salinity, and irradiance on the growth of the harmful red tide dinoflagellate *Cochlodinium polykrikoides* Margaelf (Dinophyceae). *J. Plankt. Res.* 26, 61-66.

Kim, H.G., C.K. Lee, S.G. Lee, H. Kim, and C. Park. 2001. Physico-chemical factors on the growth of *Cochlodinium polykrikoides* and nutrient utilization. *J. Korean Fish. Soc.* 34, 445-456.

Kimmerer, W.J. 1984. Selective predation and its impact on prey of *Sagitta enflata* (*Chaetognatha*). *Mar. Ecol. Progr. Ser.* 15, 55-63.

King, J.E. 1950. A preliminary report on the plankton of the west coast of Florida. *Quart. J. Fla. Acad. Sci.* 12, 109-137.

Kiorboe, T. and M. Sabatini. 1995. Scaling of fecundity, growth, and development in marine planktonic copepods. *Mar. Ecol. Progr. Ser.* 120, 285-298.

Klein, P. 1986. A simulation study of the interactions between physical and biological processes on Georges Bank. In *Georges Bank and surrounding waters*, editors R.H. Backus and D.W. Bourne, MIT Press, Cambridge, pp 395-405.

Klein Breteler, W.C., H.G. Franz, and S.R. Gonzalez. 1982. Growth and development of four calanoid copepods species under experimental and natural conditions. *Neth. J. Sea Res.* 16, 194-207.

Klein Breteler, W.C., N. Schogt, M. Baas, S. Schouten, and G.W. Kraay. 1999. Trophic upgrading of food quality by protozoans enhancing copepod growth: Role of essential lipids. *Mar. Biol.* 135, 191-198.

Klein Breteler, W.C., M. Koski, and S. Rampen. 2004. Role of essential lipids in copepod nutrition: No evidence for trophic upgrading of food quality by a marine ciliate. *Mar. Ecol. Prog. Ser.* 274, 199-208.

Kleppel, G.S., C.A. Burkart, L. Houchin, and C. Tomas. 1996. Diets of calanoid copepods on the West Florida continental shelf: Relationships between food concentration, food composition and feeding activity. *Mar. Biol.* 127, 209-217.

Knauer, G.A. and J.H. Martin. 1972. Mercury in a marine food chain. *Limnol. Oceanogr.* 17, 868-876.

Kranz, S.A., D. Sultemeyer, K.-U. Richter, and B. Rost. 2009. Carbon acquisition by *Trichodesmium*: The effect of pCO₂ and diurnal changes. *Limnol. Oceanogr.* 54, 548-559.

Kudela, R.M., J. Ryan, M. Blakely, J. Lane and T. Peterson. 2008. Linking the physiology and ecology of *Cochlodinium* to better understand harmful algal bloom events: A comparative approach. *Harm. Alg.* 7, 278-292.

Langdon, C. 1988. On the causes of interspecific differences in the growth-irradiance relationship for phytoplankton. II. A general review. *J. Plankt. Res.* 10, 1291-1312.

Lauritano, C., Y. Carotenuto, G. Procaccini, J.T. Turner, and A. Ianora. 2013. Changes in expression of stress genes in copepods feeding upon a non-brevetoxin-producing strain of the dinoflagellate *Karenia brevis*. *Harm. Algae* 16, 63-73.

Lavrentyev, P.J., W.S. Gardner, and J.R. Johnson. 1997. Cascading trophic effects on aquatic nitrification: Experimental evidence and potential implications. *Aquat. Microb. Ecol.* 13, 161-175.

Lenes, J.M., J.J. Walsh, D.B. Otis, and K.L. Carder. 2005. Iron fertilization of *Trichodesmium* off the west coast of Barbados: A one-dimensional numerical model. *Deep-Sea Res.* 52, 1021-1041.

Lenes, J.M., B.P. Darrow, J.J. Walsh, J.K. Jolliff, F.R. Chen, R.H. Weisberg, and L. Zheng. 2012. A 1-D simulation analysis of the development and maintenance of the 2001 red tide of the ichthyotoxic dinoflagellate *Karenia brevis* on the West Florida shelf. *Cont. Shelf Res.* 41, 92-110.

Lenes, J.M., J.J. Walsh, and B.P. Darrow. 2013. Simulating cell death in the termination of *Karenia brevis* blooms: Implications for predicting aerosol toxicity vectors to humans. *Mar. Ecol. Progr. Ser.* 493, 71-81.

Lester, K.M., C.A. Heil, M.B. Neely, D.N. Spence, S. Murasko, T.L. Hopkins, T.T. Sutton, S.E. Burghart, R.N. Bohrer, A.W. Remsen, G.A. Vargo, and J.J. Walsh. 2008. Zooplankton and *Karenia brevis* in the Gulf of Mexico. *Cont. Shelf Res.* 28, 99-111.

Liu, H., M.J. Dagg, C.-J. Wu, and K.-P. Chiang. 2005. Mesozooplankton consumption of microplankton in the Mississippi River plume, with special emphasis on planktonic ciliates. *Mar. Ecol. Progr. Ser.* 268, 133-144.

Liu, Y., R.H. Weisberg, C. Hu, and L. Zheng. 2011a. Trajectory forecast as a rapid response to the Deepwater Horizon oil spill. In *Monitoring and Modeling the Deepwater Horizon Oil Spill: A Record-Breaking Enterprise*, editors Y. Liu, A. MacFadyen, Z.-G. Ji, and R.H. Weisberg, AGU Geophys. Mon. Ser. 195, 153-165.

Liu, Y., R.H. Weisberg, C. Hu, C. Kovach, and R. Riethmüller 2011b. Evolution of the Loop Current system during the Deepwater Horizon oil spill event as observed with drifters and satellites. In *Monitoring and Modeling the Deepwater Horizon Oil Spill: A Record-Breaking Enterprise*, editors Y. Liu, A. MacFadyen, Z.-G. Ji, and R.H. Weisberg, AGU Geophys. Mon. Ser. 195, 91-101.

Lombard, F., A. Sciandra, and G. Gorsky. 2005. Influence of body mass, food concentration, temperature, and filtering activity on the oxygen uptake of the appendicularian *Oikopleura dioica*. *Mar. Ecol. Progr. Ser.* 301, 149-158.

Lombard, F., L. Legendre, M. Picheral, A. Sciandra, and G. Gorsky. 2010. Prediction of ecological niches and carbon export by appendicularians using a new multispecies ecophysiological model. *Mar. Ecol. Progr. Ser.* 398, 109-125.

Lombard, F., L. Guidi, and T. Kiorboe. 2013. Effect of type and concentration of ballasting particles on sinking rate of marine snow produced by the appendicularian *Oikopleura dioica*. *PLOS One* 8, e75676, 1-6.

Lopez-Urrutia, A., R.P. Harris, and T. Smith. 2004. Predation by calanoid copepods on the appendicularian *Oikopleura dioica*. *Limnol. Oceanogr.* 49, 303-307.

Lynn, D.H., J.C. Roff, and R.R. Hopcroft. 1991. Annual abundance and biomass of aloricate ciliates in tropical neritic waters off Kingston, Jamaica. *Mar. Biol.* 110, 437-448.

Magana, H.A., and T.A. Villareal. 2006. The effect of environmental factors on the growth rate of *Karenia brevis* (Davis) G. Hansen and Moestrup. *Harm. Alg.* 5, 192-198.

Mauchline, J. 1998. The biology of calanoid copepods. *Advan. Mar. Biol.* 33, 1-710.

Mayzaud, P., V. Tivelli, J.M. Bernard, and O. Roche-Mayzaud. 1998. Feeding in the copepods *Acartia tonsa*, *Centropages typicus*, and *Temora longicornis*. *J. Mar. System.* 15, 483-493.

McDaniel, L.D., J. Basso, E. Pulster, and J.H. Paul 2015. Sand patties provide evidence for the presence of *Deepwater Horizon* oil on the beaches of the West Florida shelf. *Mar. Poll. Bull.* (in press).

Mellor, G.L. and T. Yamada. 1974. A hierarchy of turbulence closure models for planetary boundary layers. *J. Atm. Sci.* 31, 1791-1806.

Mille-Pagaza, S. and J. Carillo-Laguna. 1999. Los quetognatos (Chaetognatha) del banco de Campeche en abril-mayo de 1986. *Rev. Biol. Trop.* 47, 1-9 (1999).

Mioni, C.E., A.M. Howard, J.M. DeBruyn, N.G. Bright, M.R. Twiss, B.M. Applegate, and S.W. Wilhelm. 2003. Characterization and field trials of a bioluminescent bacterial reporter of iron bioavailability. *Mar. Chem.* 83, 31-46.

Moller, H. and H.U. Rissgard. 2007. Feeding, bioenergetics, and growth in the common jellyfish *Aurelia aurita* and two hydromedusae *Sarsia tubulosa* and *Aequorea vitrina*. *Mar. Ecol. Progr. Ser.* 346, 167-177.

Mulkana, M. S. and T. D. McIlwain. 1973. The seasonal occurrence and abundance of *Chaetognatha* in Mississippi Sound. *Gulf Res. Rep.* 4, 264-271.

Mullin, M., P.R. Sloan, and R.W. Eppley. 1966. Relationship between carbon content, cell volume, and area in phytoplankton. *Limnol. Oceanogr.* 11, 307-311.

Nelson, D.M. and Q. Dortch. 1996. Silicic acid depletion and silicon limitation in the plume of the Mississippi River: Evidence from kinetic studies in spring and summer. *Mar. Ecol. Progr. Ser.* 136, 163-178.

Nicolaisen, M.H., J. Worm, N.O. Jorgensen, M. Middelboe, and O. Nybroe. 2012. Proteinase production in *Pseudomonas fluorescens* ON2 is affected by carbon sources and allows surface-attached but not planktonic cells to utilize proteins for growth in lake water. *FEMS Microb. Ecol.* 80, 168-178.

Nielsen, T.G. and T. Kiorboe. 1994. Relationship of zooplankton biomass and production in a temperate coastal ecosystem. 2. Ciliates. *Limnol. Oceanogr.* 39, 508-519.

Nimer, N.A., D. Iglesias-Rodriguez, and M.J. Merrett. 2008. Bicarbonate utilization by marine phytoplankton species. *J. Phycol.* 33, 625-631.

Nival, S., M. Pagano, and P. Nival. 1990. Laboratory study of the spawning rate of *Centropages typicus*: Effect of fluctuating food environments. *J. Plank. Res.* 12, 535-547.

Nour El-Din, N.M. and J.A. Al-Kayat. 2001. Impact of industrial discharges on the zooplankton community in the Messaieed industrial area, Qatar (Persian Gulf). *Intern. J. Environ. Studies* 58, 173-184.

O'Brien, J.J. and J.S. Wroblewski. 1973. A simulation of the mesoscale distribution of the lower marine trophic levels off West Florida. *Invest. Pesq.* 37, 193-244.

Ogawa, H. and E. Tanoue. 2003. Dissolved organic matter in oceanic waters. *J. Oceanogr.* 59, 129-147.

Ohman, M.D. and R.A. Snyder. 1991. Growth kinetics of the omnivorous oligotrich ciliate *Strombidium* sp. *Limnol. Oceanogr.* 36, 922-935.

Okamoto, O.K., L. Shao, J.W. Hastings, and P. Colepicolo. 1999. Acute and chronic effects of toxic metals on viability, encystment, and bioluminescence in the dinoflagellate *Gonyaulax polyedra*. *Comp. Bio. Phys. Part C* 123, 75-83.

Ostgaard, K., I. Eide, and A. Jensen. 1984. Exposure of phytoplankton to Ekofisk crude oil. *Mar. Environ. Res.* 11, 183-200.

Ou, L., D. Wang, B. Huang, H. Hong, Y. Qi, and S. Lu. 2008. Comparative study of phosphorus strategies of three typical harmful algae in Chinese coastal waters. *J. Plank. Res.* 30,

1997-1017.

Ozhan, K., S.M. Miles, H. Gao, and S. Bargu. 2014. Relative phytoplankton growth response to physically and chemically dispersed South Louisiana sweet crude oil. *Envir. Mon. Assess.* 186, 3941-3956.

Paasche, E. 1980. Silicon content of five marine plankton diatom species measured with a rapid filter method. *Limnol. Oceanogr.* 25, 474-480.

Pace, M.L., J.J. Cole, S.R. Carpenter, and J.F. Kitchell. 1980. Trophic cascades revealed in diverse systems. *Trends Ecol. Evol.* 14, 483-488.

Paffenhofer, G.-A. and S.C. Knowles. 1980. Omnivourness in marine planktonic copepods. *J. Plank. Res.* 2, 355-366.

Paffenhofer, G.-A. 1984. Food ingestion by the marine planktonic copepod *Paracalanus* in relation to abundance and size distribution of food. *Mar. Biol.* 80, 323-333.

Paine, R.T. 1980. Food webs: Linkage, interaction strength, and community infrastructure. *J. Anim. Ecol.* 49, 667-685.

Paul, J.H., D. Hollander, P. Coble, K.L. Daly, S. Murasko, D. English, J. Basso, J. Delaney, L. McDaniel, and C.W. Kovach. 2013. Toxicity and mutagenicity of Gulf of Mexico waters during and after the *Deepwater Horizon* oil spill. *Envir. Sci. Tech.* 47, 9651-9659.

Pauly, D., V. Christensen, J. Dalsgaard, R. Froese, and F.C. Torres. 1998. Fishing down marine food webs. *Science* 279, 860-863.

Pierce, D.J. and B. Mahmoudi. 2001. Near shore fish assemblages along the central west coast of Florida. *Bull. Mar. Sci.* 68, 243-270.

Pierce, E.L. 1951. The chaetognatha of the west coast of Florida. *Biol. Bull.* 100, 206-228.

Pomeroy, L.R., J.E. Sheldon, W.M. Sheldon, and F. Peters. 1995. Limits to growth and respiration of bacterioplankton in the Gulf of Mexico. *Mar. Ecol. Progr. Ser.* 117, 259-268.

Porch, C.E., S.C. Turner, and M.J. Schirripa. 2007. Reconstructing the commercial landings of red snapper in the Gulf of Mexico from 1872 to 1963. In *Red snapper ecology and fisheries in the Gulf of Mexico*, editors W.F. Patterson, J.H. Cowan, G.R. Fitzhugh, and D.L. Nieland, *Amer. Fish. Soc. Symp.* 60, 337-353.

Putt, M. and D.K. Stoecker. 1989. An experimentally determined carbon: volume ratio for marine "oligotrichous" ciliates from estuarine and coastal waters. *Limnol. Oceanogr.* 34, 1097-1103.

Reeve, M.R. 1964. Studies on the seasonal variation of the zooplankton in a marine subtropical inshore environment. *Bull. Mar. Sci. Gulf Carib.* 14, 103-122.

Reeve, M.R. and M.A. Walter. 1972. Conditions of culture, food size selection, and the effects of temperature and salinity on the growth and generation time in *Sagitta hispida* Conant. *J. Exp. Mar. Biol. Ecol.* 9, 191-200.

Reeve, M.R. 1980. Comparative experimental studies on the feeding of chaetognaths and ctenophores. *J. Plank. Res.* 2, 381-393.

Renan, X., T. Brule, T. Colas-Marrufo, Y. Hauyon, and C. Deniel. 2001. Preliminary results on the reproductive cycle of the black grouper, *Mycteroperca bonaci*, from the southern Gulf of Mexico. *Proc. Gulf Carib. Fish. Inst.* 52, 1-14.

Riebesell, U. 2004. Effects of CO₂ enrichment on marine phytoplankton. *J. Oceanogr.* 60, 719-729.

Riley, G.A. 1967. Mathematical model of nutrient conditions in coastal waters. *Bull. Bingham Oceanogr. Coll.* 19, 72-80.

Rogerson, A. and J. Berger. 1981. Effects of crude oil and petroleum-degrading micro-organisms on the growth of freshwater and soil protozoa. *J. Gen. Microbiol.* 124, 53-59.

Rost, B., U. Riebesell, and S. Burkhardt. 2003. Carbon acquisition of bloom-forming marine phytoplankton. *Limnol. Oceanogr.* 48, 55-67.

Rost, B., K.-U. Richter, U. Riebesell, and P.J. Hansen. 2006. Inorganic carbon acquisition in red tide dinoflagellates. *Plant, Cell, Environ.* 29, 810-822.

Sato, R., Y. Tanaka, and T. Ishimaru. 2003. Species-specific house productivity of appendicularians. *Mar. Ecol. Progr. Ser.* 259, 163-172.

Saunders, R.P. and D.A. Glenn. 1969. Diatoms. *Memoirs of the Hourglass Cruises, Volume 1, Part III*, pp 1-119.

Sautour, B. and J. Castel. 1995. Comparative spring distribution of zooplankton in three macrotidal European estuaries. *Hydrobiologia* 311, 139-151.

Shiah, F.-K., and H.W. Ducklow. 1994. Temperature and substrate regulation of bacterial abundance, production, and specific growth rate in Chesapeake Bay, USA. *Mar. Ecol. Progr. Ser.* 103, 297-308.

Skoog, A., B. Biddanda, and R. Benner. 1999. Bacterial utilization of dissolved glucose in the upper water column of the Gulf of Mexico. *Limnol. Oceanogr.* 44, 1635-1633.

Smith, S.L. and P.V. Lane. 1985. Laboratory studies of the marine copepod *Centropages typicus*: Egg production and development rates. *Mar. Biol.* 85, 153-162.

Sommer, F., T. Hansen, H. Feuchtmayr, B. Santer, N. Tokle, and U. Sommer. 2003. Do calanoid copepods suppress appendicularians in the coastal ocean? *J. Plank. Res.* 25, 869-871.

Sommer, F., and U. Sommer. 2004. Del N-15 signatures of marine mesozooplankton and seston size fractions in Kiel Fjord, Baltic Sea. *J. Plank. Res.* 26, 495-500.

Speekman, C.L., C.J. Hyatt, and E.J. Buskey. 2006. Effects of *Karenia brevis* diet on RNA:DNA ratios and egg production of *Acartia tonsa*. *Harm. Algae* 5, 693-704.

Stauber, J.L. and S.W. Jeffrey. 1988. Photosynthetic pigments in fifty-one species of marine diatoms. *J. Phycol.* 24, 158-172.

Steidinger, K.A. and J. Williams. 1970. Dinoflagellates. *Mem. Hourglass Cruises, Vol. II*, pp 1-251.

Steidinger, K.A., G.A. Vargo, P.A. Tester, and C.R. Tomas. 1998. Bloom dynamics and physiology of *Gymnodinium breve* with emphasis on the Gulf of Mexico. In *Physiological ecology of harmful algal blooms*, editors D.M. Anderson, A.D. Cembella, and G.M. Hallegraeff, Springer Verlag, Berlin, pp 135-153.

Stibor, H., O. Vadstein, B. Lippert, W. Roederer, and Y. Olsen. 2004. Calanoid copepods and nutrient enrichment determine population dynamics of the appendicularian *Oikopleura dioica*: A mesocosm experiment. *Mar. Ecol. Progr. Ser.* 270, 209-215.

Stommel, H. and A. Leetma. 1972. Circulation on the continental shelf. *Proc. Nat. Acad. Sci.* 69, 3380-3384.

Strom, S.L. and T.A. Morello. 1998. Comparative growth rates and yields of ciliates and heterotrophic dinoflagellates. *J. Plankt. Res.* 20, 571-584.

Taft, J.L., W.R. Taylor, and J.J. McCarthy. 1975. Uptake and release of phosphorus by phytoplankton in the Chesapeake Bay estuary, USA. *Mar. Biol.* 33, 21-32.

Tang, K.W., and M. Taal. 2005. Trophic modification of food quality by heterotrophic protists: Species-specific effects on egg production and egg hatching. *J. Exp. Mar. Biol. Ecol.* 318, 85-98.

Thompson, P.A., M. Guo, and P.J. Harrison. 1992. Effects of variation in temperature. I. On the biochemical composition of eight species of marine phytoplankton. *J. Phycol.* 28, 481-488.

Tiselius, P. 1989. Contribution of aloricate ciliates to the diet of *Acartia clausi* and *Centropages hamatus* in coastal waters. *Mar. Ecol. Progr. Ser.* 56, 49-56.

Tonnesson, K. and P. Tiselius 2005. Diet of chaetognaths *Sagitta setosa* and *S. elegans* in relation to prey abundance and vertical distribution. *Mar. Ecol. Progr. Ser.* 289, 177-190.

Tortell, P.D., M.T. Maldando, J. Granger, and N.M. Price. 1999. Marine bacteria and biogeochemical cycling of iron in the oceans. *FEMS Microb. Ecol.* 29, 1-11.

Tortell, P.D., G.H. Rau, and F.M. Morel. 2000. Inorganic carbon acquisition in coastal Pacific phytoplankton communities. *Limnol. Oceanogr.* 45, 1485-1500.

Troedsson, C., M.E. Frischer, J.C. Nejstgaard, and E.M. Thompson. 2002. Molecular quantification of differential ingestion and particle trapping rates by the appendicularian *Oikopleura dioica* as a function of prey size and shape. *Limnol. Oceanogr.* 52, 416-427.

Turner, J.T. 1984. Zooplankton feeding ecology: Contents of fecal pellets of the copepods *Temora turbinata* and *T. stylifera* from continental shelf and slope waters near the mouth of the Mississippi River. *Mar. Biol.* 82, 73-83.

Turner, J.T. 1987. Zooplankton feeding ecology: Contents of fecal pellets of the copepod *Centropages velificatus* near the mouth of the Mississippi River. *Biol. Bull.* 173, 377-386.

Turner, J.T., and P.A. Tester. 1997. Toxic marine phytoplankton, zooplankton grazers, and pelagic food webs. *Limnol. Oceanogr.* 42, 1203-1214.

Turner, J.T., V. Roncalli, P. Camarillo, C. Dell'Aversano, E. Fattorusso, L. Tartaglione, Y. Carotenuto, G. Romano, F. Espoisto, A. Miraldo, and A. Ianora. 2012. Biogeographical effects of the Gulf of Mexico red tide dinoflagellate *Karenia brevis* on Mediterranean copepods. *Harm. Algae* 16, 63-73.

Uye, S.-I. and K. Takamatsu. 1990. Feeding interactions between planktonic copepods and red-tide flagellates from Japanese coastal waters. *Mar. Ecol. Progr. Ser.* 59, 9-107.

Uye, S.-I. and H. Shimauchi. 2005. Population biomass, feeding, respiration and growth rates, and carbon budget of the scyphomedusa *Aurelia aurita* in the Inland Sea of Japan. *J. Plank. Res.* 27, 237-248.

Vargas, C.A. and H.E. Gonzalez. 2004. Plankton community structure and carbon cycling in a coastal upwelling system. I: Bacteria, microprotozoans, and phytoplankton in the diets of copepods and appendicularians. *Aquat. Microb. Ecol.* 34, 151-164.

Vargo, G.A. and D. Howard-Shambrott. 1990. Phosphorus requirements in *Ptychodiscus brevis*: cell phosphorus, uptake and growth requirements. In *Toxic marine phytoplankton*, editors E. Graneli, B. Sundstrom, L. Edler, and D.M. Anderson, Elsevier, Amsterdam, pp 324-329.

Verity, P.G. 1991. Measurement and simulation of prey uptake by marine planktonic ciliates fed plastidic and aplastidic nanoplankton. *Limnol. Oceanogr.* 36, 729-750.

Vrede, K., M. Heldal, S. Norland, and G. Bratbak. 2002. Elemental composition (C, N, P) and cell volume of exponentially growing and nutrient-limited bacterioplankton. *Appl. Environ. Microbiol.* 68, 2965-2971.

Waggett, R.J., D.R. Hardison, and P.A. Tester. 2012. Toxicity and nutritional inadequacy of *Karenia brevis*: Synergistic mechanisms disrupt top-down grazer control. *Mar. Ecol. Progr. Ser.*

Ser. 444, 15-30.

Walsh, J.J., D.A. Dieterle, M.B. Meyers, and F.E. Muller-Karger. 1989. Nitrogen exchange at the continental margin: A numerical study of the Gulf of Mexico. *Prog. Oceanogr.* 23, 245-301.

Walsh, J.J., D.A. Dieterle, F.E. Muller-Karger, K. Aagaard, A.T. Roach, T.E. Whittle, and D. Stockwell. 1997. CO₂ cycling in the coastal ocean. II. Seasonal organic loading to the Canadian Basin from source waters south of Bering Strait. *Cont. Shelf Res.* 17, 1-36.

Walsh, J.J., B. Penta, D.A. Dieterle, and W. P. Bissett. 2001. Predictive ecological modeling of harmful algal blooms. *Hum. Ecol. Risk Assess.* 7, 1369-1383.

Walsh, J.J. and K.A. Steidinger. 2001. Saharan dust and Florida red tides: the cyanophyte connection. *J. Geophys. Res.* 106, 11597-11612.

Walsh, J.J., R.H. Weisberg, D.A. Dieterle, H. He, B.P., Darrow, J.K. Jolliff, K.M. Lester, G.A. Vargo, G.J. Kirkpatrick, K.A. Fanning, T.T. Sutton, A.E. Jochens, D.C. Biggs, B. Nababan, C. Hu, and F.E. Muller-Karger. 2003. The phytoplankton response to intrusions of slope water on the West Florida shelf: Models and observations. *J. Geophys. Res.* 108, 3190, doi: 10.1029/2002JC001406.

Walsh, J.J., J.K. Jolliff, B.P. Darrow, J.M. Lenes, S.P. Milroy, D. Remsen, D.A. Dieterle, K.L. Carder, F.R. Chen, G.A. Vargo, R.H. Weisberg, K.A. Fanning, F.E. Muller-Karger, E. Shinn, K.A. Steidinger, C.A. Heil, J.S. Prospero, T.N. Lee, G.J. Kirkpatrick, T.E. Whittle, D.A. Stockwell, C.R. Tomas, T.A. Villareal, A.E. Jochens, and P.S. Bontempi. 2006. Red tides in the Gulf of Mexico: where, when, and why. *J. Geophys. Res.* 111, C11003, doi:10.1029/2004JC002813.

Walsh, J.J., R.H. Weisberg, J.M. Lenes, F.R. Chen, D.A. Dieterle, L. Zheng, K.L. Carder, G.A. Vargo, J.A. Havens, E. Peebles, D.J. Hollander, R. He, C.A. Heil, B. Mahmoudi, and J.H. Landsberg. 2009. Isotopic evidence for dead fish maintenance of Florida red tides, with implications for coastal fisheries over both source regions of the West Florida shelf and within downstream waters of the South Atlantic Bight. *Prog. Oceanogr.* 80, 51-73.

Walsh, J.J., K.A. Steidinger, J.M. Lenes, F.R. Chen, R.H. Weisberg, L. Zheng, J.H. Landsberg, G.A. Vargo, and C.A. Heil. 2011. Imprudent fishing harvests and consequent trophic cascades on the West Florida shelf over the last half century: A harbinger of increased human deaths from paralytic shellfish poisoning along the southeastern United States, in response to oligotrophication? *Cont. Shelf Res.* 31, 891-911.

Walsh J.J., J.M. Lenes, B. Darrow, A. Parks, R.H. Weisberg, L. Zheng, C. Hu, B. Barnes, K.L. Daly, G. Brooks, W. Jeffrey, R. Snyder and D. Hollander. 2015a. A simulation analysis of the plankton fate of the *Deepwater Horizon* oil spills in 2010-2011. *Cont. Shelf. Res.* 107, 50-68.

Walsh, J.J., J.M. Lenes, R.H. Weisberg, L. Zheng, C. Hu, K.A. Fanning, R. Snyder, and J. Smith. 2015b. More surprises in the global greenhouse: Human health impacts from recent toxic marine algal aerosol formations, due to centennial alteration of world-wide coastal food webs. *Mar. Poll. Bull.* (submitted).

Ward, B.B. 1996. Nitrification and denitrification: Probing the nitrogen cycle in aquatic environments. *Microb. Ecol.* 32, 247-261.

Wardlaw, T., E.W. Johansson, and M. Hodge. 2006. Pneumonia: The forgotten killer of children. UNICEF/WHO, pp 1-42.

Weisberg, R.H., and R. He. 2003. Local and deep-ocean forcing contributions to anomalous water properties on the West Florida shelf. *J. Geophys. Res.* 108, doi:10.1029/2002JC001407.

Weisberg, R.H., L. Zheng, Y. Liu, C. Lembke, J.M. Lenes, and J.J. Walsh. 2014. Why no red tide was observed on the West Florida continental shelf in 2010. *Harm. Algae* 38, 119-126.

Weisberg, R.H., L. Zheng, Y. Liu, S. Murawski, C. Hu, and J. Paul. 2015a. Did Deepwater Horizon hydrocarbons transit to the West Florida continental shelf? *Deep-Sea Res., Part II*, doi:10.1016/j.dsr2.2014.02.002 (in press).

Weisberg, R.H., L. Zheng and E. Peebles. 2015b. Gag grouper larvae pathways on the West Florida Shelf. *Cont. Shelf Res.* (in press).

Wiadnyana, N.N. and F. Rassoulzadegan. 1989. Selective feeding of *Acartia clausi* and *Centropages typicus* on microzooplankton. *Mar. Ecol. Progr. Ser.* 53, 37-45.

Wiebe, P.H., S. Boyd, and J.L. Cox. 1975. Relationships between zooplankton displacement volume, wet weight, dry weight, and carbon. *Fish. Bull.* 73, 777-786.

Williams, P.M. and E.R. Druffel. 1987. Radiocarbon in dissolved organic matter in the central North Pacific Ocean. *Nature* 330, 246-248.

Wroblewski, J.S. and J.G. Richman. 1987. The nonlinear response of plankton to wind mixing events – implications for larval fish survival. *J. Plank. Res.* 9, 103-123.

Wu, C.-H., H.-U. Dahms, E.J. Buskey, J.R. Strickler, and J.-S. Hwang. 2010. Behavioral interactions of the copepod *Temora turbinata* with potential ciliate prey. *Zoo. Stud.* 49, 157-168.

Zhang, R., B. Liu, S.C. Lau, J.S. Ki, and P.Y. Qian. 2007. Particle-attached and free-living bacterial communities in a contrasting marine environment: Victoria Harbor, Hong Kong. *FEMS Microbiol. Ecol.* 61, 496-508.

Table 1. Model ecophysiological parameters of Bacterioplankton: ammonifiers (*Pseudomonas* Ba); nitrifiers (*Nitrosomonas* Bn); Phytoplankton: diatoms (*Skeletonema* Ps, *Rhizosolenia* Pr); dinoflagellates (*Karenia* Pk, *Cochlodinium* Pc); autotrophic microflagellates (*Isochrysis* Pm); heterotrophic microflagellates (*Paraphysomonas* Ph); diazotrophs (*Trichodesmium* Pt); and Zooplankton: ciliates (*Strobilidium* Zs); tunicates (*Oikopleura* Zo); copepods (*Temora* Zt, *Centropages* Zc); chaetognaths (*Sagitta* Zg); and medusae (*Aurelia* Za)

	Ba	Bn	Ps	Pr	Pk	Pc	Pm	Ph	Pt	Zs	Zo	Zt	Zc	Zg	Za
<u>Growth rates at 30°C (day⁻¹)</u>	1.5 ¹	2.0 ¹	3.4 ²	1.9 ³	1.0 ⁴	1.6 ⁵	3.1 ⁶	3.1	0.9 ⁷	7.0 ⁸	3.0 ⁹	0.5 ¹⁰	0.6 ¹⁰	0.2 ¹¹	0.2 ¹²
<u>Metabolic thermal Q₁₀</u>	3.4 ¹³	3.4 ¹³	2.0 ¹⁴	2.0 ¹⁴	2.0 ¹⁴	2.0 ¹⁴	2.0 ¹⁴	2.0	2.0 ¹⁴	2.6 ¹⁵	1.7 ¹⁶	3.0 ¹⁷	3.0 ¹⁷	2.7 ¹⁸	2.8 ¹⁹
<u>Half-saturation constant (umol l⁻¹)</u>															
<u>Silicate</u>	-	-	0.8 ²⁰	1.5 ²¹	-	-	-	-	-	-	-	-	-	-	-
<u>Nitrate</u>	-	-	0.5 ²²	1.7 ²²	0.4 ²³	0.6 ²⁴	0.3 ²⁵	-	-	-	-	-	-	-	-
<u>Ammonium</u>	-	0.3 ²⁵	0.5 ²⁵	1.7 ²⁶	0.4 ²⁵	0.6 ²⁴	0.2 ²⁵	-	-	-	-	-	-	-	-
<u>DON</u>	1.5 ²⁶	-	2.0 ²⁵	2.5 ²⁵	1.0 ²³	1.5 ²⁴	1.5 ²⁶	-	-	-	-	-	-	-	-
<u>Phosphate</u>	-	0.1	0.3 ²⁷	0.3 ²⁸	0.2 ²⁹	0.5 ²⁴	0.2 ²⁵	-	0.1 ³⁰	-	-	-	-	-	-
<u>DOP</u>	0.5 ²⁵	-	1.0 ³¹	1.0 ²⁵	0.4 ²⁹	1.0 ²⁴	1.0 ²⁵	-	0.2 ²⁵	-	-	-	-	-	-
<u>Carbon</u>	0.1 ³²⁻³³	0.1	0.5 ³⁴⁻³⁵	1.2 ³⁶	1.4 ^{34,37}	1.4 ^{34,37}	0.3 ³⁸	1.5	2.5 ³⁸⁻³⁹	8 ⁴⁰	4 ⁴¹	8 ⁴²⁻⁴³	8 ⁴²⁻⁴³	2 ⁴⁴	1 ⁴⁵
<u>Iron (pmol l⁻¹)</u>	10 ⁴⁶⁻⁴⁷	10	5 ³⁰	5 ³⁰	5 ³⁰	5 ³⁰	5 ³⁰	5.0	500 ³⁰	-	-	-	-	-	-
<u>Light saturation (uE m⁻² sec⁻¹)</u>	-	-	225 ²⁶	190 ²⁶	65 ²⁶	400 ²⁴	275 ²⁶	-	400 ³⁰	-	-	-	-	-	-
<u>C/chl weight ratio</u>	-	-	110 ⁴⁸⁻⁴⁹	53 ⁴⁸⁻⁴⁹	30 ²⁵	100 ²⁵	200 ²⁵	-	100 ²⁵	-	-	-	-	-	-
<u>Hg content (ng Hg g⁻¹ dw)</u>						207 ⁵⁰									

¹Goldman and Dennett (2000); ²Langdon (1988); ³Furnas (1991); ⁴Magana and Villareal (2006); ⁵Kim et al. (2004); ⁶Thompson et al. (1992); ⁷Carpenter and Roenneberg (1995); ⁸Strom and Morello (1998); ⁹Troedsson et al. (2002); ¹⁰Chisholm and Roff (1990); ¹¹Kimmerer (1984); ¹²Uye and Shimauchi (2005); ¹³Shiah and Ducklow (1994); ¹⁴Banse (1982); ¹⁵Nielsen and Kiorboe (1994); ¹⁶Gorsky et al. (1987); ¹⁷Huntley and Lopez (1992); ¹⁸Reeve and Walter (1972); ¹⁹Hansson (1997); ²⁰Davis et al. (1978); ²¹Nelson and Dortch (1996); ²²Eppley et al. (1969); ²³Steidinger et al. (1998); ²⁴Kudela et al. (2008); ²⁵Lenes et al. (2012); ²⁶Walsh et al. (2001); ²⁷Ou et al. (2008); ²⁸Kim et al. (2001); ²⁹Vargo and Howard-Shambrot (1990); ³⁰Lenes et al. (2005); ³¹Taft et al. (1975); ³²Azam and Hudson (1981); ³³Button et al. (1992); ³⁴Caperon and Smith (1978); ³⁵Rost et al. (2003); ³⁶Tortell et al. (2000); ³⁷Rost et al. (2006); ³⁸Burns and Beardall (1987); ³⁹Kranz et al. (2009); ⁴⁰Verity (1991); ⁴¹Acuna and Kiefer (2000); ⁴²Dagg and Grill (1980); ⁴³Mayzaud et al. (1998); ⁴⁴Reeve (1980); ⁴⁵Moller and Rissgard (2007); ⁴⁶Tortell et al. (1999); ⁴⁷Mioni et al., 2003; ⁴⁸Mullin et al. (1966); ⁴⁹Stauber and Jeffrey (1988); ⁵⁰Knauer and Martin (1972).

Table 2. Pre-cascade and post-cascade summer budgets of the prey pools of carbon (umol C L⁻¹), potentially available to copepod omnivores and other consumers in a planktonic biomass pyramid, over the 5-m isobath of the inner central West Florida shelf between 1948-1973 and 2001-2002.

	1948-1973	2001-2002
Primary producers:		
Mircoflagellates	0.2 ¹	0.2 ²
Diatoms	3.3 ³	8.8 ⁴⁻⁵
Other dinoflagellates	75.8 ⁶	-
HABs	12.5	125.0
Total:	91.8	135.0
Ciliate omnivores	66.7	5.5 ⁷
Tunicate omnivores	0.1	2.3 ⁹
Meroplankton larval herbivores	7.7 ⁸	129.0 ⁹
Total:	74.5	136.8
Copepod Omnivores	18.3	1.1 ⁹
Larval fish predators	0.0012 ¹⁰	0.0001
Chaetognath predators	0.4000 ¹¹⁻¹³	0.0140
Medusa predators	0.4420 ¹⁴	0.0167 ¹⁵
Total:	0.8432	0.0308

¹(Walsh and Steidinger, 2001); ²(Heil et al., 2004); ³(Saunders and Glenn, 1969); ⁴(Bledsoe and Phlips, 2000); ⁵(Jurado et al., 2007); ⁶(Steidinger and Williams, 1970); ⁷(Lynn et al., 1991); ⁸(Hopkins, 1977); ⁹(Badylak and Phlips, 2008); ¹⁰(Houde and Chitty, 1976); ¹¹(Pierce, 1951); ¹²(Reeve, 1964); ¹³(Mulkana and McIlwain, 1973); ¹⁴(Burke, 1975); ¹⁵(Graham, 2002).

Table 3. Boundary conditions of zooplankton (umol C l⁻¹) at the 5-m and 45-m isobaths during 1965-1966.

	Jan	Feb	Mar	Apr	May	Jun	Jul	Aug	Sep	Oct	Nov	Dec
<i>Temora</i>												
5-m	0.26	0.19	0.13	0.26	0.58	0.28	0.27	0.13	0.14	0.28	0.65	0.48
45-m	0.01	0.01	0.01	0.01	0.01	0.01	0.01	0.01	0.01	0.01	0.01	0.01
<i>Centropages</i>												
5-m	0.70	0.50	0.30	0.70	1.50	0.80	0.70	0.50	0.40	0.80	1.70	1.30
45-m	0.20	0.10	0.10	0.20	0.40	0.20	0.20	0.10	0.10	0.20	0.40	0.30
<i>Oikopleura</i>												
5-m	0.03	0.02	0.02	0.03	0.07	0.04	0.03	0.02	0.02	0.04	0.08	0.06
45-m	0.01	0.01	0.01	0.01	0.01	0.01	0.01	0.01	0.01	0.01	0.01	0.01
<i>Strobilidium</i>												
5-m	26.70	2.30	20.23	6.70	14.50	2.30	66.70	6.70	24.40	4.40	6.70	24.40
45-m	2.40	2.00	2.40	4.30	1.90	0.90	1.00	0.40	2.70	1.50	0.60	0.70

Table 4. Boundary conditions of zooplankton (umol C l⁻¹) at the 5-m and 45-m isobaths during 2001-2002.

	Jan	Feb	Mar	Apr	May	Jun	Jul	Aug	Sep	Oct	Nov	Dec
<i>Temora</i>												
5-m	0.02	0.02	0.02	0.01	0.02	0.03	0.05	0.06	0.10	0.02	0.03	0.05
45-m	0.01	0.01	0.01	0.01	0.01	0.01	0.01	0.01	0.01	0.01	0.01	0.01
<i>Centropages</i>												
5-m	0.01	0.01	0.01	0.01	0.03	0.08	0.06	0.03	0.04	0.05	0.06	0.01
45-m	0.02	0.01	0.01	0.01	0.01	0.01	0.02	0.01	0.02	0.01	0.01	0.02
<i>Oikopleura</i>												
5-m	0.03	0.04	0.02	0.01	0.06	0.08	0.05	0.02	0.12	0.12	0.04	0.04
45-m	0.01	0.01	0.01	0.01	0.01	0.01	0.01	0.01	0.01	0.01	0.01	0.01
<i>Strobilidium</i>												
5-m	2.67	0.23	2.23	0.67	1.45	0.23	6.94	0.67	2.44	0.44	0.67	2.44
45-m	0.24	0.20	0.24	0.43	0.19	0.09	0.10	0.04	0.27	0.15	0.06	0.07

Table 5. Boundary conditions of zooplankton (umol C l⁻¹) at the 5-m and 45-m isobaths during 2010-2011.

	Jan	Feb	Mar	Apr	May	Jun	Jul	Aug	Sep	Oct	Nov	Dec
<i>Temora</i>												
5-m	0.01	0.01	0.01	0.01	0.01	0.01	0.01	0.01	0.01	0.01	0.01	0.01
45-m	0.01	0.01	0.01	0.01	0.01	0.01	0.01	0.01	0.01	0.01	0.01	0.01
<i>Centropages</i>												
5-m	0.01	0.01	0.01	0.01	0.01	0.01	0.01	0.01	0.01	0.01	0.01	0.01
45-m	0.02	0.01	0.01	0.01	0.01	0.02	0.02	0.05	0.03	0.02	0.01	0.02
<i>Oikopleura</i>												
5-m	0.01	0.01	0.01	0.01	0.01	0.01	0.01	0.01	0.01	0.01	0.01	0.01
45-m	0.01	0.01	0.01	0.01	0.01	0.01	0.01	0.01	0.01	0.01	0.01	0.01
<i>Strobilidium</i>												
5-m	2.67	0.23	2.23	0.67	1.45	0.23	6.94	0.67	2.44	0.44	0.67	2.44
45-m	0.24	0.20	0.24	0.43	0.19	0.09	0.10	0.04	0.27	0.15	0.06	0.07

Table 6. Computed seasonal plankton maxima ($\mu\text{mol C l}^{-1}$) on the 20-m isobath over the last 46 years (1965-2011) of fishing and oil spill perturbations of the West Florida shelf.

	1965	1966	2001	2002	2010	2011
Diazotroph-based food chain						
<i>Trichodesmium</i> [1 August]	17.00	14.00	20.00	27.00	7.00	14.00
<i>Karenia</i> [1 October]	91.00	90.00	177.00	77.00	8.00	100.00
Diatom-based food chain						
<i>Skeletonema</i> [1 April]	0.30	0.30	0.80	0.70	0.70	0.70
<i>Temora</i> [1 May]	0.48	0.46	0.02	0.02	0.01	0.02
<i>Rhizosolenia</i> [1 September]	4.30	0.50	1.60	0.60	1.10	2.70
<i>Centropages</i> [1 November]	0.60	0.55	0.06	0.06	0.01	0.01
Flagellate-based food chain						
Sum of <i>Synechococcus</i> +						
<i>Paraphysomonas</i> [1 June]	1.34	1.34	1.30	1.45	1.31	1.39
<i>Oikopleura</i> [1 June]	0.12	0.11	0.14	0.08	0.02	0.02
<i>Strobilidium</i> [1 July]	5.00	19.00	2.00	2.20	1.30	2.20
Dinoflagellate shunt						
<i>Cochlodinium</i> [1 January]	0.30	0.20	0.20	3.50	0.10	4.00

List of figure legends

Figure 1. Locations of decadal validation data of a 2-D numerical model along the cross-shelf section off Sarasota, Florida during 1965-2011, in relation to both prior ship-board observations obtained during: 1965-1967 [HOURGLASS stations over the same ECOHAB sampling grid]; 1998 [Mote sections]; 1998-2000 [NEGOM surveys]; 1998-2001 [ECOHAB cruises]; 1999-2000 [RSMAS/AOML], and the *Deepwater Horizon* (DWH) oil spill in 2010. Additional data were obtained during repeated C-IMAGE samplings during 2010-2011 near the Panama City cross-shelf survey in 2000.

Figure 2. Nutrient depth profiles of (A) phosphate, (B) nitrate, (C) ammonium, and (D) silicate at the shelf-break off Panama City, Florida, during NEGOM observations in August 2000, compared to those of more recent C-IMAGE stations DSH08, DSH09, and DSH10, occupied in the same WFS region during August 2010.

Figure 3. A time series of the observed mean weekly surface abundances (cells l^{-1}) of *Karenia brevis* during 1957-2011 along the 5-m isobath between Cedar Key and Naples, FL, with gray panels of the time periods of the three model scenarios of A) pre-cascade in 1965-1966, B) cascade in 2001-2002, and C) post *Deepwater Horizon* oil spills in 2010-2011.

Figure 4. The daily simulated surface concentrations on the 20-m isobath of nitrate and ammonium during A) 1965-1966, B) 2001-2002, and C) 2010-2011, under a scenario of fast nitrification rates of oxidation of simulated ammonium stocks, in relation to observed pools of dissolved nitrogen during intense upwellings in B) 1998 vs. 1999 and C) 2010 vs. 2011.

Figure 5. Simulated surface biomasses of nitrogen-fixers *Trichodesmium* and harmful algal blooms *Karenia brevis* on the 20-m isobath during 2001-2002. Open circles are FWRI observations.

Figure 6. The simulated standing stocks on the WFS 20-m isobath of large diatoms *Rhizosolenia* spp. [panels A, C, E] in relation to validation data (open circles) between 1965-1967 (Saunders and Glenn, 1969) and (open triangles) during 1999-2002 (Jurado et al., 2007). Similarly, model results for computed stocks of small diatoms *Skeletonema costatum* [panels B, D, F] are compared with other observations (open circles) in 1965-1967 (Saunders and Glenn, 1969).

Figure 7. The daily simulated surface distributions of the relatively non-toxic dinoflagellate *Cochlodinium polykrikoides* above the 20-m isobath of the WFS during A) 1965-1966, B) 2001-2002, and C) 2010-2011 in relation to FWRI observations on the shelf and within estuarine waters that year (O).

Figure 8. The daily simulated sum of surface ammonifying and nitrifying bacteria populations above the 20-m isobath of the WFS during A) 1965-66, B) 2001-02, and C) 2010-11 in relation to available (Jones et al., 2010) observations (O).

Figure 9. The daily simulated surface distributions of the tunicate herbivore *Oikopleura* (A, C, E) and ciliate omnivore *Strobilidium* (B, D, F) above the 20-m isobath of the WFS during A - B) 1965-66, C - D) 2001-02, and E - F) 2010-11 in relation to available (FWRI; Lester et al., 2008; Walsh et al., 2015) observations (O). Note scale change in panel B.

Figure 10. The daily simulated surface distributions of the copepods *Temora* (A, C, E) and *Centropages* (B, D, F) above the 20-m isobath of the WFS during A - B) 1965-66, C - D) 2001-02, and E - F) 2010-11 in relation to validation (FWRI; Lester et al., 2008; Walsh et al., 2015) data (O). Note scale changes.

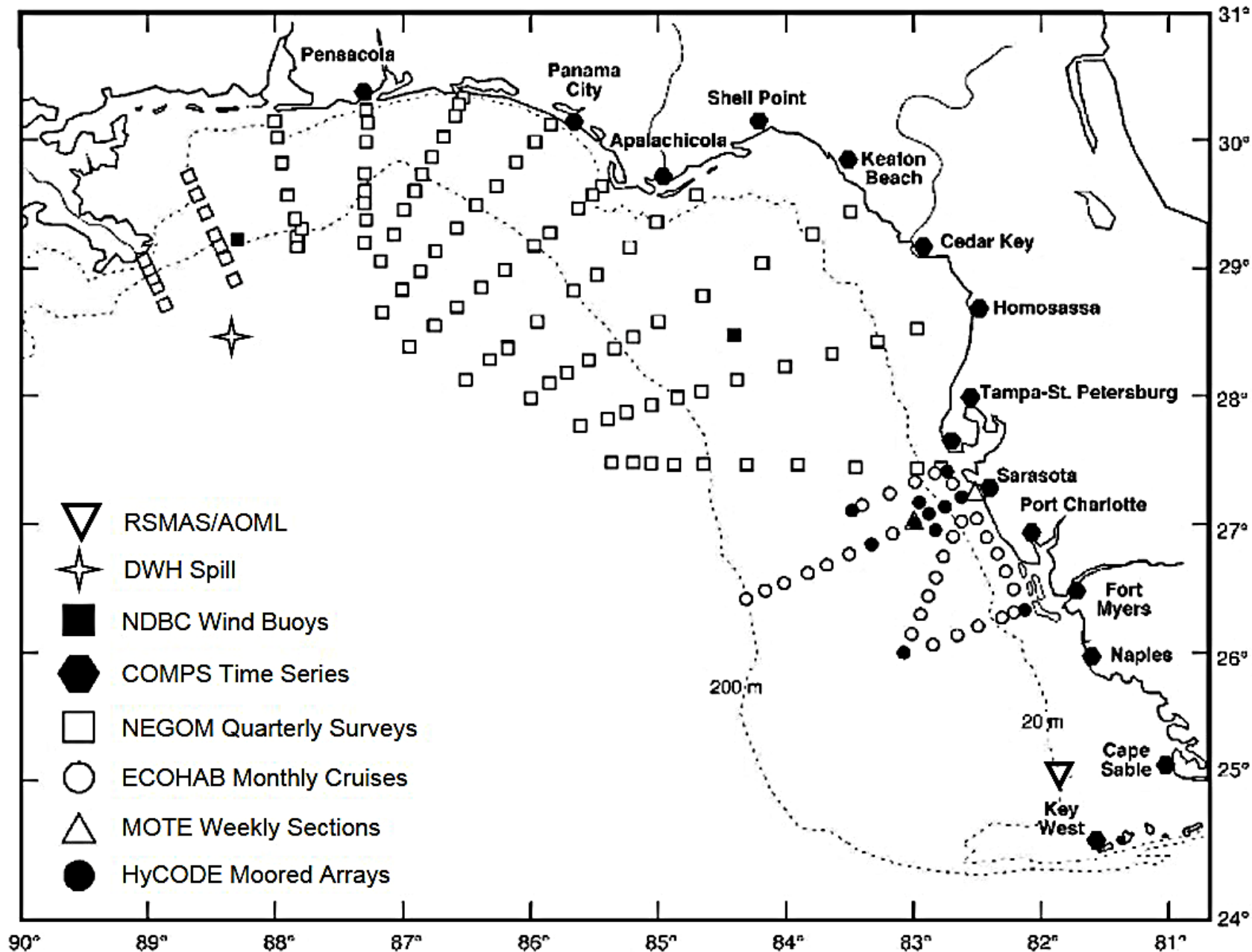


Figure 1.

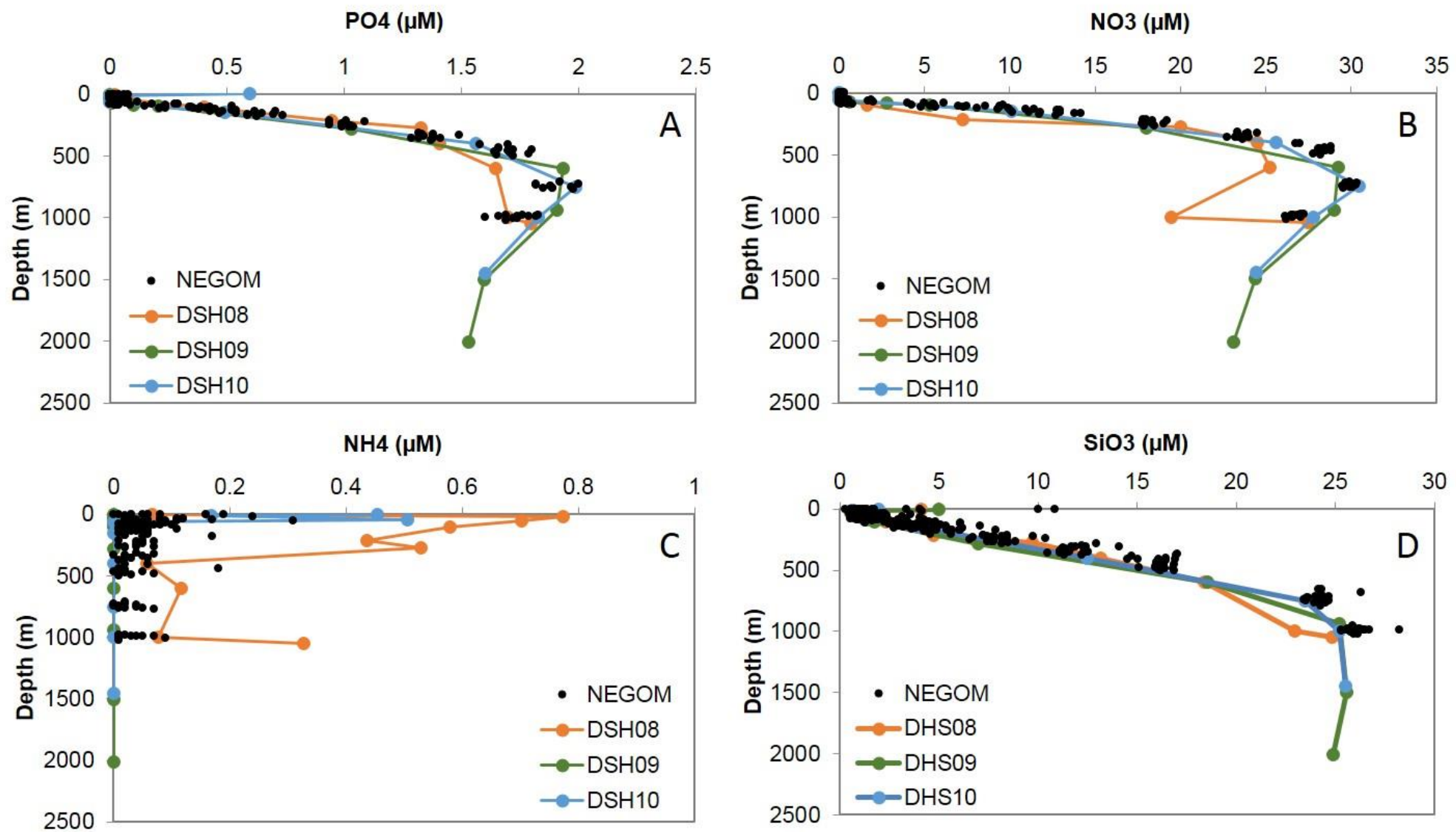


Figure 2.

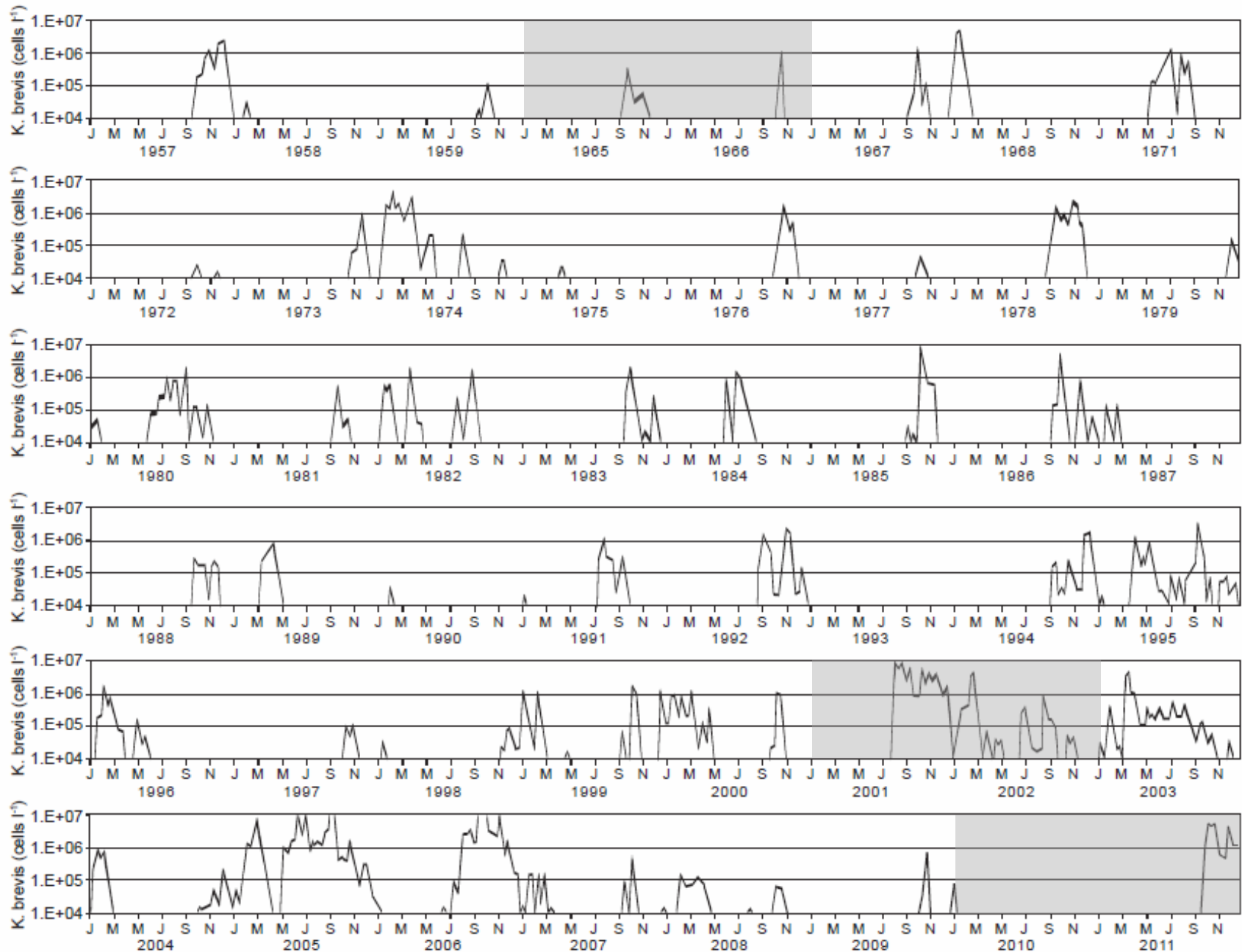


Figure 3.

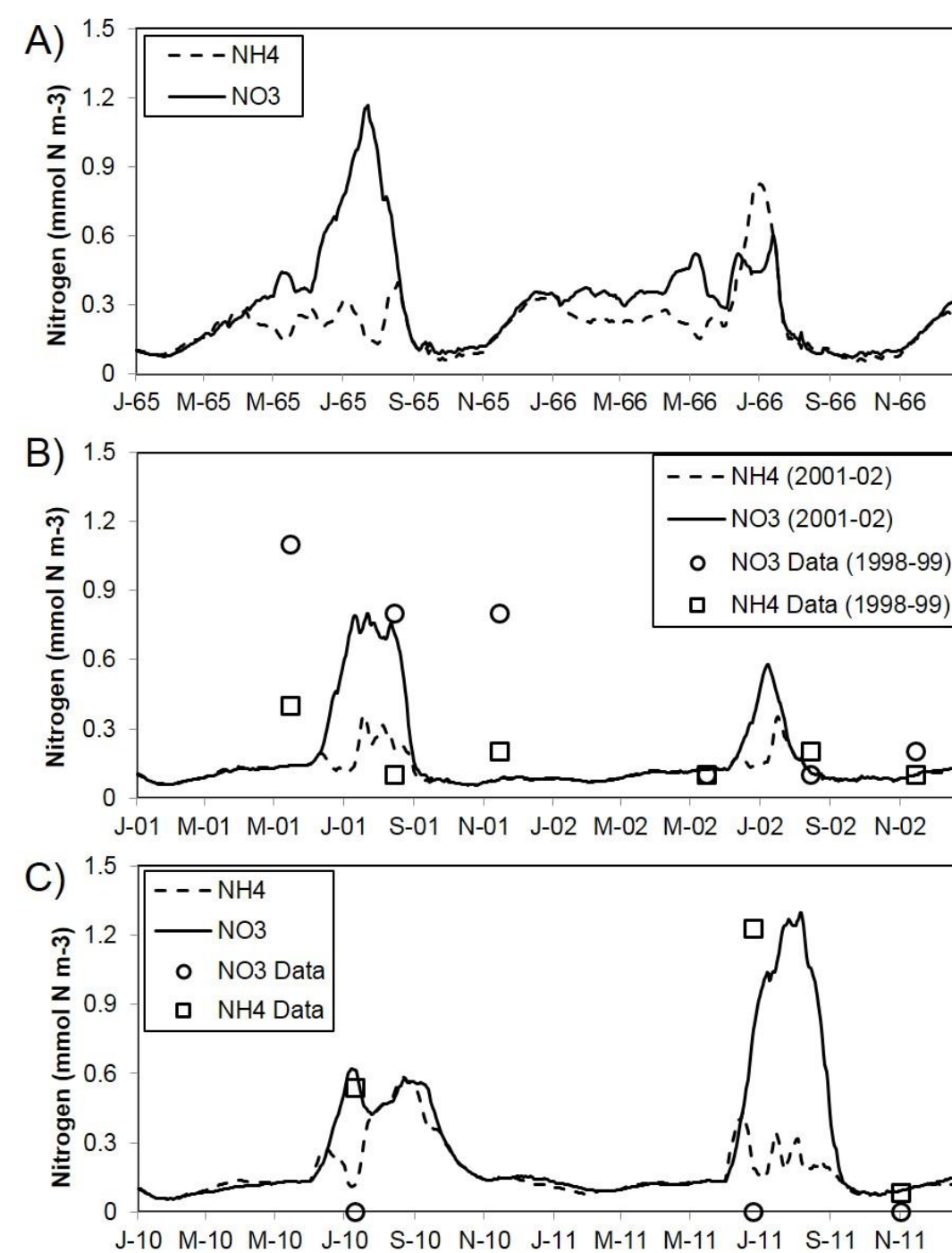


Figure 4.

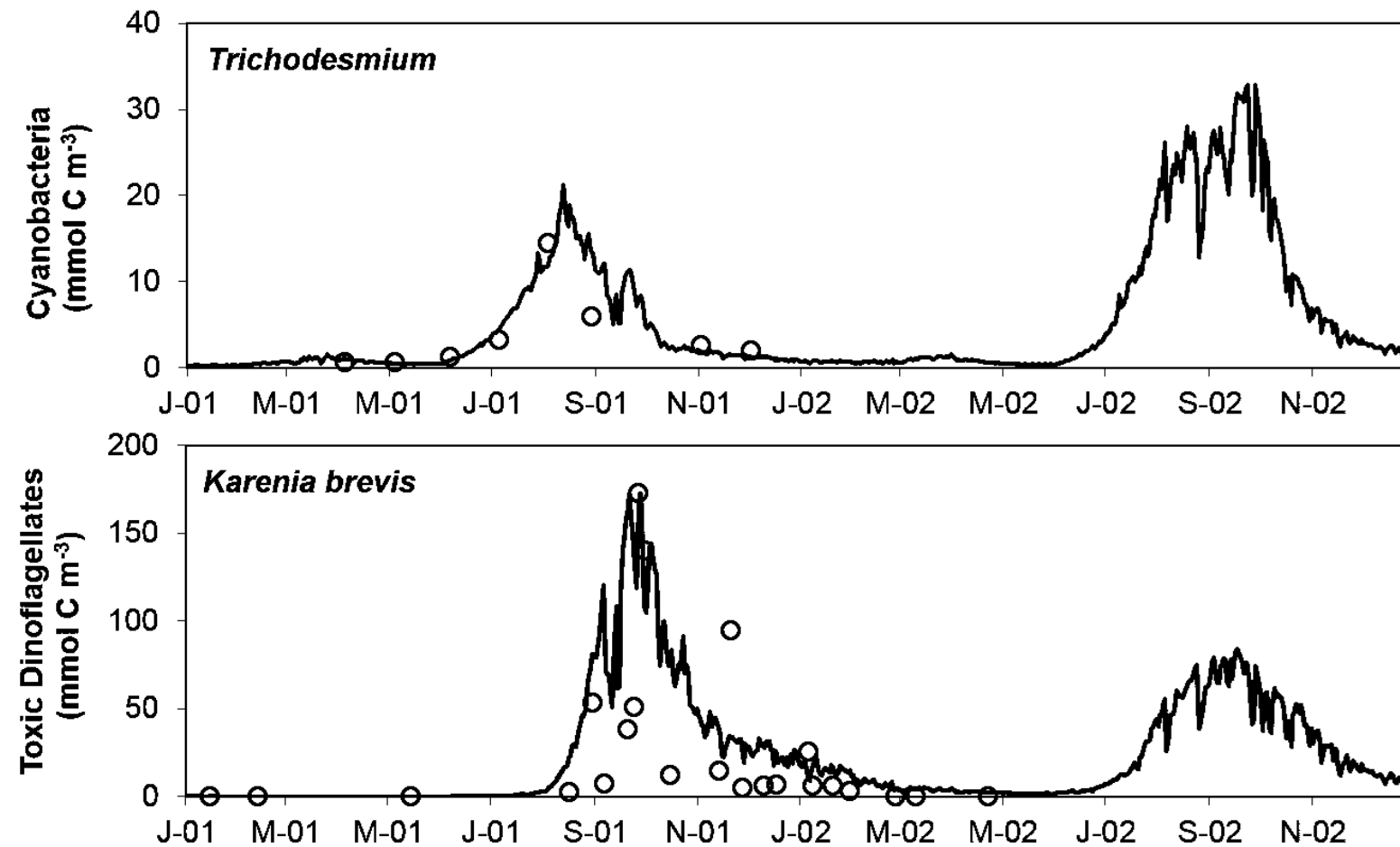


Figure 5.

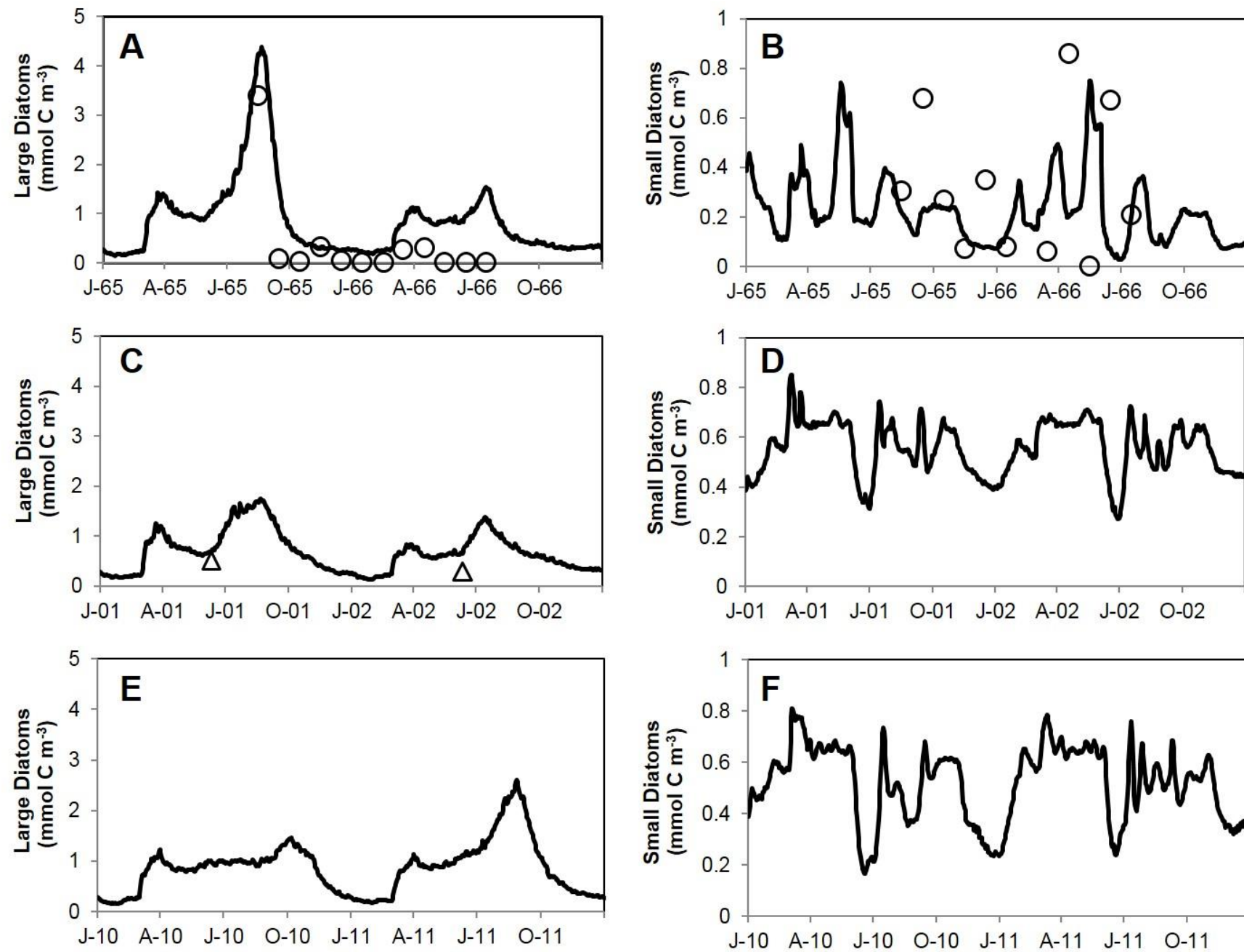


Figure 6.

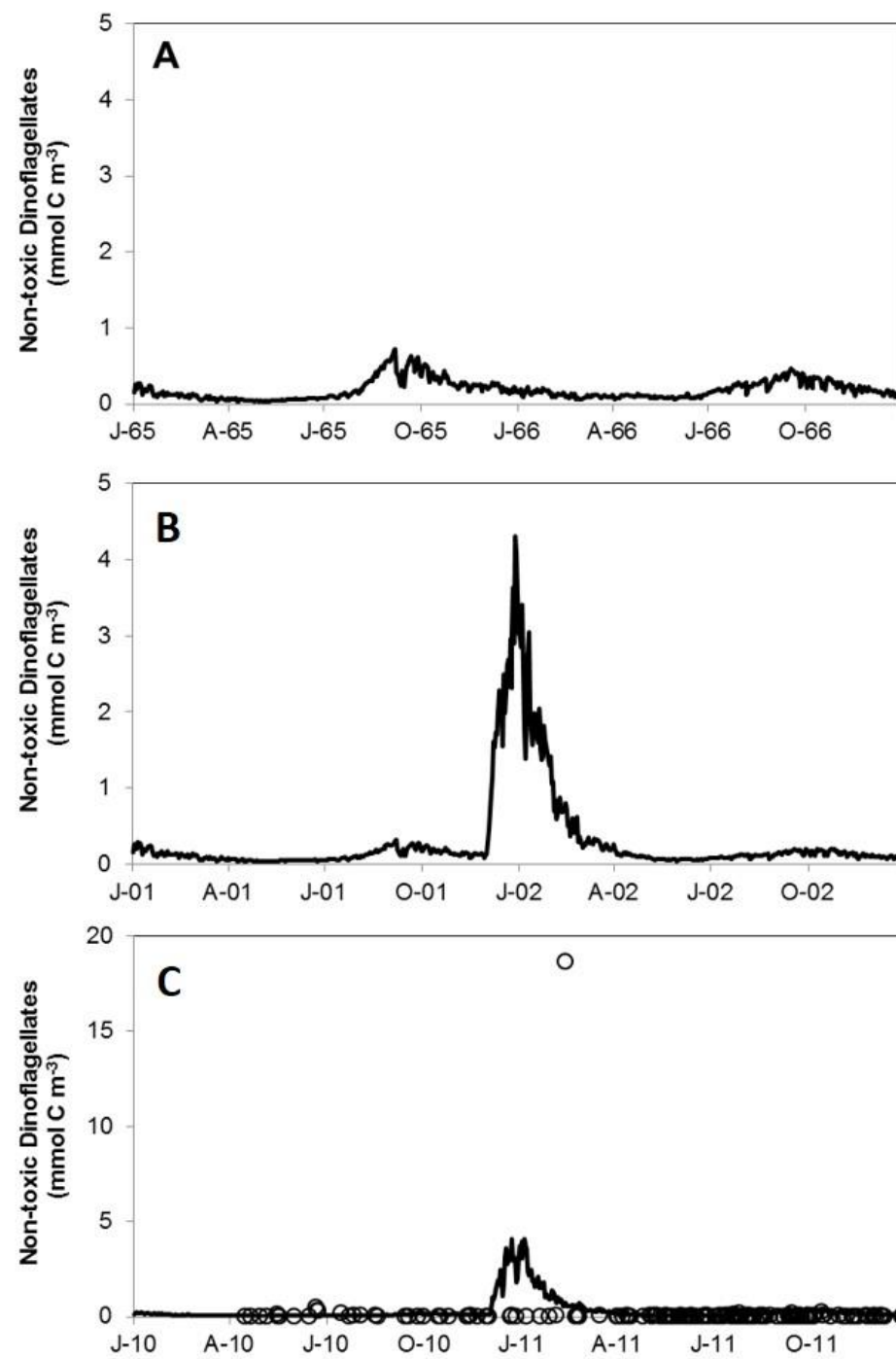


Figure 7.

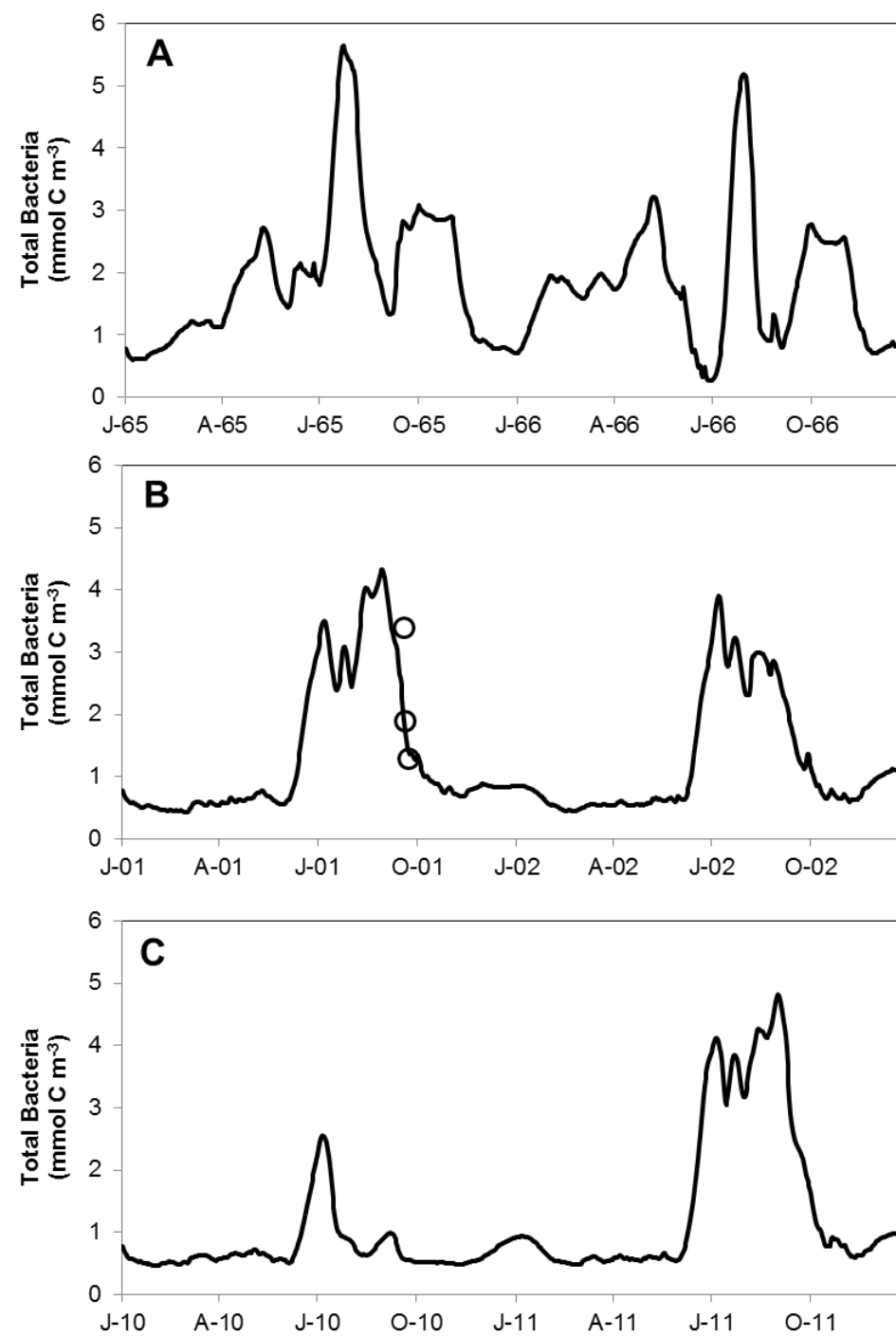


Figure 8.

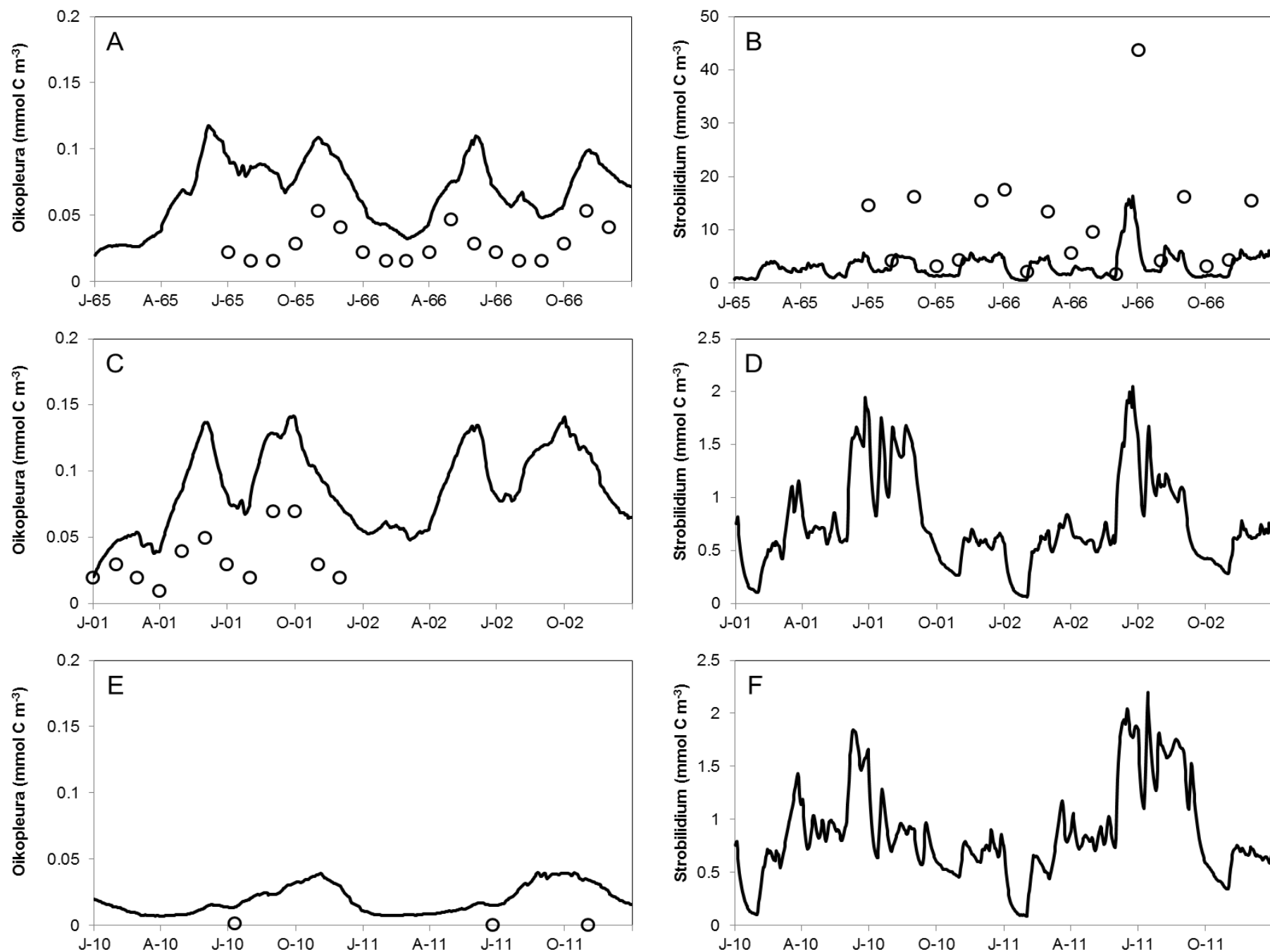


Figure 9.

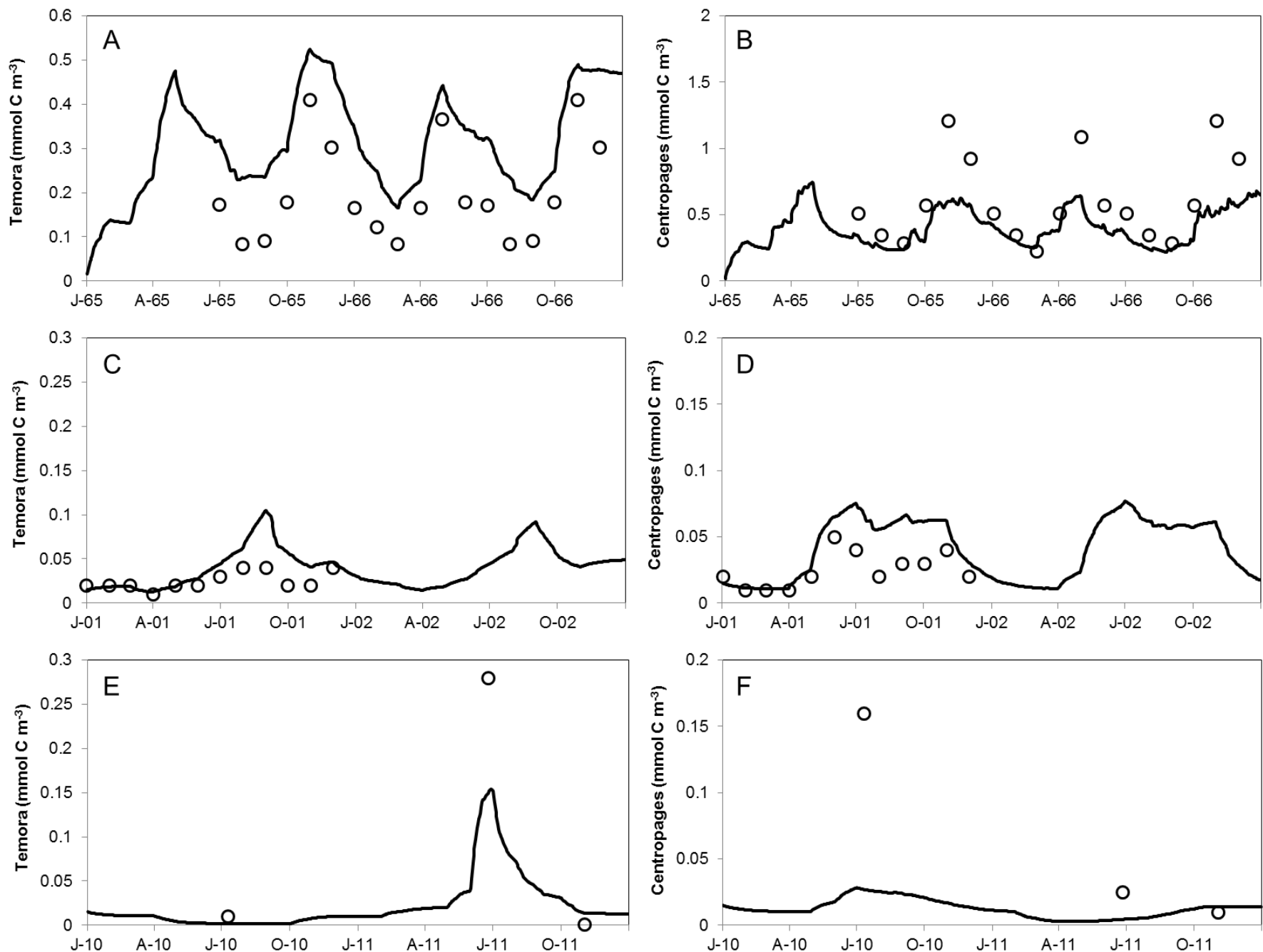


Figure 10.